Published in final edited form as:
Toxicon. 2012 March 15; 59(4): 529–546. doi:10.1016/j.toxicon.2011.07.016.

Development of a sea anemone toxin as an immunomodulator for therapy of autoimmune diseases

Victor Chi[1], **Michael W. Pennington**[2], **Raymond S. Norton**[3], **Eric Tarcha**[4], **Luz Londono**[4], **Brian Sims-Fahey**[4], **Sanjeev K. Upadhyay**[1], **Jonathan T. Lakey**[1], **Shawn Iadonato**[4], **Heike Wulff**[5], **Christine Beeton**[6], and **K. George Chandy**[1]

[1]Department of Physiology and Biophysics, and Department of Surgery, UC Irvine, Irvine, CA 92697

[2]Peptides International, 11621 Electron Drive, Louisville, KY 40299 USA

[3]Medicinal Chemistry and Drug Action, Monash Institute of Pharmaceutical Sciences, Monash University, 399 Royal Parade, Parkville 3052, Australia

[4]Kineta Inc. 307 Westlake Ave North, Seattle, WA 98199

[5]Department of Pharmacology, UC Davis, Davis, CA 95616

[6]Department of Molecular Physiology and Biophysics, Baylor College of Medicine, Houston, TX 77030

Abstract

Electrophysiological and pharmacological studies coupled with molecular identification have revealed a unique network of ion channels—Kv1.3, KCa3.1, CRAC (Orai1 + Stim1), TRPM7, Cl_{swell}—in lymphocytes that initiates and maintains the calcium signaling cascade required for activation. The expression pattern of these channels changes during lymphocyte activation and differentiation, allowing the functional network to adapt during an immune response. The Kv1.3 channel is of interest because it plays a critical role in subsets of T and B lymphocytes implicated in autoimmune disorders. The ShK toxin from the sea anemone *Stichodactyla helianthus* is a potent blocker of Kv1.3. ShK-186, a synthetic analog of ShK, is being developed as a therapeutic for autoimmune diseases, and is scheduled to begin first-in-man phase-1 trials in 2011. This review describes the journey that has led to the development of ShK-186.

Ion channels were discovered in the immune system in 1984 when it became possible to record electrical signals from single lymphocytes (DeCoursey et al., 1984; Matteson and Deutsch, 1984). It is now clear that five types of ion channels—the potassium channels Kv1.3 and KCa3.1, the Ca^{2+}-release activating Ca^{2+} (CRAC) channel encoded by the Orai and STIM1 (stromal interacting protein 1) genes, TRPM7 involved in magnesium homeostasis, and Cl_{swell} (swelling-activated chloride channel)—constitute a network in T lymphocytes that is vital for cellular homeostasis, activation and differentiation (Cahalan and Chandy, 2009). The coalescence of Kv1.3, KCa3.1 and CRAC channels at the immunological synapse (Beeton et al., 2006; Lioudyno et al., 2008; Nicolaou et al., 2007; Panyi et al., 2004) during antigen presentation has the potential to generate local ionic accumulation or depletion, and to mediate trans-synaptic signaling by assembling into molecular aggregates or signalosomes (Cahalan and Chandy, 2009). These channels also regulate the Ca^{2+} signaling required for lymphocyte activation by maintaining a balance between Ca^{2+} influx and K^+ efflux (Cahalan and Chandy, 2009). Of particular interest is the Kv1.3 channel, which plays a critical functional role in effector-memory (T_{EM}) cells and class-switched memory B cells that are implicated in diverse autoimmune diseases (Beeton et al., 2006; Wulff et al., 2003; Wulff et al., 2004). Potent and selective channel blockers of

Kv1.3 have been developed, which are effective in diverse animal models of immunological disorders (Beeton et al., 2005; Beeton et al., 2006; Norton et al., 2004; Pennington et al., 2009; Schmitz et al., 2005; Wulff and Pennington, 2007).

1. The clinical problem – autoimmune diseases

Nearly 80 different autoimmune disorders are known, affecting more than 125 million people worldwide. Autoimmune diseases involve virtually every organ system in the body including joints (e.g. rheumatoid arthritis [RA], ankylosing spondylitis), the central nervous system (multiple sclerosis [MS]), endocrine organs (type-1 diabetes mellitus [T1DM], Hashimoto's thyroiditis) (Leyendeckers et al., 2002) and skin (psoriasis). Tissue destruction is mediated by autoreactive (self-reactive) immune cells. The frequency of autoreactive lymphocytes (e.g. against myelin antigens in the central nervous system) is the same in healthy individuals as in patients with autoimmune diseases. However, healthy individuals do not develop autoimmune diseases because these potentially self-destructive cells are suppressed and maintained in a quiescent naïve state by regulatory T cells. Once an autoreactive T lymphocyte is triggered to proliferate and/or escapes regulation, the presence of the autoantigen in the body causes the cell to undergo repeated stimulation until it changes into a terminally differentiated cell called a T_{EM}-effector, which contributes to tissue damage. Disease-associated autoreactive T cells in patients with MS (specific for myelin antigens), T1DM (specific for insulin and GAD65 antigens), RA (synovial T cells) or psoriasis are T_{EM}-effector cells (Beeton et al., 2006; Fasth et al., 2004; Friedrich et al., 2000; Lovett-Racke et al., 1998; Miyazaki et al., 2008; Rus et al., 2005; Viglietta et al., 2002; Vissers et al., 2004; Wulff et al., 2003). Autoreactive B cells similarly differentiate upon repetitive autoantigen stimulation into class-switched memory B cells, which are implicated in MS (Corcione et al., 2004), Hashimoto's thyroiditis (Leyendeckers et al., 2002), Sjorgen's syndrome (Hansen et al., 2002), and systemic lupus erythematosis (Dorner and Lipsky, 2004; Jacobi et al., 2003). A therapeutic approach that mutes or eliminates T_{EM}-effectors and class-switched memory B cells without compromising the protective immune response mediated by other lymphoid subsets would have significant advantages over current therapies that broadly suppress the entire immune response.

2. Why target K^+ channels in immune cells?

K^+ channels promote calcium influx in lymphocytes

Calcium signaling is essential for lymphocytes to activate, synthesize and secrete cytokines (or antibodies), migrate *in vivo*, and proliferate. In the case of T cells, antigen binding to the T-cell receptor causes the generation of IP_3, which releases Ca^{2+} from the ER Ca^{2+} store (Figure 1). Depletion of the ER store triggers an ER protein called STIM1 to cluster under the plasma membrane and activate Ca^{2+} influx through CRAC channels formed from Orai1 subunits (Lioudyno et al., 2008; Luik et al., 2008; Park et al., 2009; Penna et al., 2008). The influx of Ca^{2+} raises the cytosolic Ca^{2+} concentration from a resting value of 50–100 nM into the low micromolar range (Figure 1). Ca^{2+} influx is sustained by the counterbalancing efflux of K^+ through Kv1.3 or KCa3.1 (Figure 1). The relative contribution of Kv1.3 and KCa3.1 varies according to their relative expression level, which changes depending on the state of differentiation and activation of lymphocytes (Cahalan and Chandy, 2009; Chandy et al., 2004). This differential K^+ channel expression pattern allows Ca^{2+} signaling to be targeted specifically in different lymphocyte subsets.

Kv1.3 and KCa3.1 are differentially expressed during lymphocyte activation and differentiation

The activation and differentiation scheme for human T and B lymphocytes is shown in Figure 2. Naïve $CD4^+$ or $CD8^+$ human T cells differentiate into long-lived central memory

(T_{CM}) T cells (main memory pool), which then differentiate into T_{EM} cells on repeated stimulation. T cells at each stage activate into effectors—naïve-effector, T_{CM}-effector, T_{EM}-effector—when they encounter antigen. CCR7, a chemokine receptor required for homing to lymph nodes, is expressed on the cell surface of naïve and T_{CM} cells as well as their respective effectors, whereas, T_{EM} cells and T_{EM}-effectors do not express CCR7 (Sallusto et al., 1999). Therefore, we divide human T cells into $CCR7^+$ (naïve and T_{CM}) and $CCR7^-$ (T_{EM}) subsets. Human B cells undergo a similar differentiation process. Naïve human B cells (IgD^+CD27^-) differentiate into early memory B cells (IgD^+CD27^+), and on repeated stimulation these cells differentiate into class-switched memory B cells (IgD^-CD27^+) that express IgG, IgA or IgE on their cell surface (Agematsu et al., 2000; Nagumo et al., 2002). For the purpose of this discussion, human B cells are divided into IgD^+ (naïve and early memory) and IgD^+ (class-switched memory) subsets.

Expression of Kv1.3 and KCa3.1 varies in $CCR7^+$ and $CCR7^-$ T cells, and IgD^+ and IgD^- B cells, as summarized in Table 1. In humans, quiescent naïve, T_{CM} and T_{EM} cells express about 300 functional Kv1.3 channels and about 10–20 KCa3.1 channels per cell (Figure 2). Their channel-expression-pattern changes upon activation into effector cells (Ghanshani et al., 2000; Wulff et al., 2003; Wulff et al., 2004). KCa3.1 expression increases to about 500 channels per cell when $CCR7^+$ T cells (naïve and T_{CM} cells) activate into effectors (naïve-effectors and T_{CM}-effectors). Activation by ionomycin alone (which triggers calcium signaling) does not up-regulate expression of KCa3.1, whereas activation by phorbol myristate acetate alone (which activates protein kinase C) increases KCa3.1 levels via transcriptional activation of Ikaros and AP-1 sites on the KCa3.1 promoter and new synthesis of KCa3.1 channel protein (Ghanshani et al., 2000). $CCR7^-$ T_{EM} cells, in contrast, up-regulate Kv1.3 to about 1500 per cell (Wulff et al., 2003) when they are activated into T_{EM}-effectors (Figure 2). This change in CCR7 expression and channel phenotype can be demonstrated *in vitro* by challenging human T cells multiple times with antigen. Repetitive antigen stimulation causes a progressive decrease of CCR7 and KCa3.1 expression and an increase in Kv1.3 levels, reflecting the differentiation from $CCR7^+$ naïve T cells into $CCR7^-$ T_{EM} cells (Wulff et al., 2003).

A similar change in K^+ channel expression pattern is seen as rat T cells differentiate from naïve to T_{EM} cells (Table 1). Quiescent naïve rat T cells from normal spleen or lymph node express fewer Kv1.3 channels (1–10 Kv1.3 per cell) than human naïve T cells and the same number of KCa3.1 channels (10–20 per cell). When activated, naïve rat T cells up-regulate both Kv1.3 (~200 /cell) and KCa3.1 (~300 /cell) and acquire a pattern similar to activated $CCR7^+$ human naïve-effector T cells (Beeton et al., 2001). Repeated antigen stimulation of rat T cells causes them to differentiate into T cells with a channel phenotype similar to human T_{EM}-effectors (~1500 Kv1.3/cell; 20–100 KCa3.1/cell) (Beeton et al., 2001). Antigen-specific rat T cell lines are $CCR7^-$ T_{EM}-effectors and exhibit the $Kv1.3^{high}$ channel pattern (Beeton et al., 2006).

In Rhesus and Sootey Mangabey monkeys, naïve, T_{CM} and T_{EM} cells express 70–125 Kv1.3 channels and 5–10 KCa3.1 channels per cell when quiescent (Table 1). Upon activation, naïve and T_{CM} cells up-regulate both Kv1.3 (250/cell) and KCa3.1 (200/cell) channels (Pereira et al., 2007), while T_{EM} cells up-regulate only Kv1.3 (~1000 Kv1.3/cell; 10–20 KCa3.1/cell). Similarly, T cells from cynomologus monkeys display an outward K^+ current with biophysical properties of Kv1.3 and sensitivity to the Kv1.3-specific inhibitor ShK-186 (data not shown).

Of clinical relevance, disease-associated autoreactive T-cell clones from patients with MS and T1DM are $CCR7^-$ T_{EM}-effectors that express high numbers of Kv1.3 (Beeton et al., 2006; Wulff et al., 2003). In patients with MS, myelin antigen-specific patient T cells were

$CCR7^-$ T_{EM}-effectors that express >1000 Kv1.3 channels per cell, whereas T cells specific for pancreatic antigens (insulin or GAD) from the same patients were $CCR7^+$ T cells and exhibited the Kv1.3 pattern of naïve/T_{CM} cells (Beeton et al., 2006). In the brains of patients with MS, $CD3^+/CD4^+/CCR7^-$ T_{EM} cells are abundant in the perivenular infiltrate and parenchymal infiltrate of the majority of MS plaques, and many of these cells stained positively for Kv1.3 (Rus et al., 2005). In patients with RA, T cells from the synovial fluid of affected joints were $CCR7^-$ T_{EM} cells with >1000 Kv1.3 channels per cell, whereas T cells from the synovial fluid of non-autoimmune osteoarthritis patients were $CCR7^+$ T cells with low numbers of Kv1.3 (Beeton et al., 2006). Synovial biopsies from affected RA joints showed the presence of $CCR7^-$ T_{EM} cells that stained positively for Kv1.3. The Kv1.3 channel is therefore an interesting target for the treatment of diverse autoimmune diseases.

The biophysical and pharmacological properties of the voltage-gated and calcium-activated K^+ channels in human B cells are identical to those of cloned Kv1.3 and KCa3.1 homotetramers and their expression pattern changes during differentiation and activation as it does in T cells (Figure 2) (Wulff et al., 2004). IgD^+ B cells (naïve and early memory), like their T-cell counterparts (naive and T_{CM} cells), up-regulate KCa3.1 upon activation, whereas IgD^- B cells (class-switched memory), like T_{EM} cells, up-regulate Kv1.3 upon activation (Wulff et al., 2004). Interestingly, quiescent class-switched memory B cells express much higher Kv1.3 levels than quiescent T_{EM} cells. It should be noted that these cells are probably not truly resting since they are enlarged in size and express other activation markers like CD86 (Wulff et al., 2004).

Pharmacological sensitivity to K^+ channel blockers parallels the K^+ channel expression pattern in lymphocytes

The switch in K^+ channel phenotype has important functional consequences in T and B cells. Kv1.3 channels regulate membrane potential and calcium signaling in resting $CCR7^+$ T cells, but when they are activated into effector cells (naïve-effector and T_{CM}-effector) KCa3.1 takes over this role (Chandy et al., 2004; Wulff et al., 2003). Consequently, selective blockers of Kv1.3 suppress activation/proliferation (^{3}H-thymidine incorporation) of $CCR7^+$ T cells (Beeton et al., 2006; Ghanshani et al., 2000; Vennekamp et al., 2004; Wulff et al., 2003), although these cells up-regulate KCa3.1 channels within 6–8 h and escape Kv1.3 blocker-inhibition while acquiring sensitivity to KCa3.1 blockade (Figure 2). By contrast, $CCR7^-$ T cells (T_{EM} and T_{EM}-effector) depend exclusively on Kv1.3 channels to provide the counterbalancing K^+ efflux needed to sustain calcium signaling in the resting and effector stages (Beeton et al., 2005; Beeton et al., 2006; Schmitz et al., 2005; Vennekamp et al., 2004; Wulff et al., 2003). These cells remain sensitive to inhibition by Kv1.3 blockers when they transit from quiescent to T_{EM}-effector cells and when T_{EM}-effectors undergo further activation (Figure 2). Pharmacological sensitivity again parallels the K^+ channel expression pattern in human B cells. KCa3.1-specific inhibitors inhibit activation/proliferation (^{3}H-thymidine incorporation) of IgD^+ B cells (naive or early memory), while Kv1.3 blockers have no effect (Wulff et al., 2004). By contrast, Kv1.3 blockers suppress the proliferation of class-switched memory B cells, while KCa3.1 inhibitors have no effect (Wulff et al., 2004).

Kv1.3 plays an important role in other immune cells

The Kv1.3 channel has also been implicated in the modulation of responses of other immune cell types. Kv1.3 expression is increased during dendritic cell maturation, and the predominant outward current in mature dendritic cells is biophysically and pharmacologically consistent with Kv1.3 (Mullen et al., 2006; Zsiros et al., 2009). Certain subsets of NK cells that engage and destroy foreign cells, also express Kv1.3 channels, and their secretion of cytolytic granules and their killing of target cells is dependent on Kv1.3-

regulation of membrane potential (Schlichter et al., 1986; Sidell et al., 1986). Kv1.3 in microglia contributes to the respiratory burst in these cells (Khanna et al., 2001) and microglia-mediated neuronal killing (Fordyce et al., 2005). Thus, Kv1.3 inhibitors such as ShK-186 may have a role in immune modulation beyond simply the T_{EM}-effector and class-switched memory B cell populations.

3. The discovery of ShK and development of ShK-186

Stichodactyla helianthus is a common species of sea anemone in the Caribbean Sea around Cuba. In 1995, Olga Castaneda, Evert Karlsson, Alan Harvey, Reto Stöcklin and their colleagues found that *Stichodactyla helianthus* extracts administered to mice by intraperitonal injection, induced hypersensitivity to touch and sound, excessive salivation, lacrimation, sweating, motor incoordination and paralysis, reminiscent of poisoning by cholinesterase inhibitors (Castaneda and Harvey, 2009; Castaneda et al., 1995). However, a whole-animal study revealed weak cholinesterase inhibitor-activity in the extracts, suggesting that these toxic symptoms were due to activity against a different molecular target. Realizing that the K^+ channel-blocking snake venom toxin dendrotoxin could produce a similar toxicity pattern via enhanced cholinergic impulses, these investigators used a screening assay based on ^{125}I-dendrotoxin binding to synaptosomes to identify a peptide, ShK, that blocked K^+ channels in cultured neurons (Castaneda et al., 1995). Soon after, Michael Pennington, William Kem, Ray Norton and their colleagues synthesized the peptide (Pennington et al., 1995), determined its three-dimensional structure (Tudor et al., 1996), and showed that ShK blocked the Kv1.3 channel in T cells with low picomolar affinity (Pennington et al., 1996).

ShK contains 35 amino acids including six cysteines that form three disulfide bonds (Figure 3) (Pohl et al., 1995). ShK blocks Kv1.3 with an IC_{50} of ~10 pM (Kalman et al., 1998), but it also blocks two other channels with picomolar potency (Kv1.1, Kv1.6) and three others (Kv1.2, Kv3.2 and KCa3.1) with nanomolar potency (Table 1). It was therefore important to develop ShK analogs with improved selectivity for Kv1.3 over the other channels. As a first step, an Ala scan of non-Cys residues was utilized to identify ShK residues required for interaction with Kv1.3 (Arg^{11}, His^{19}, Ser^{20}, Lys^{22}, Tyr^{23}, Arg^{24}); these residues were found to be clustered on one surface of the peptide (Pennington et al., 1996; Rauer et al., 1999) (Figure 4). Complementary mutagenesis and double mutant cycle analysis were then used to characterize the ShK-binding site on Kv1.3 (Kalman et al., 1998; Lanigan et al., 2002). ShK binds to a shallow vestibule at the outer mouth of the Kv1.3 channel pore where it interacts predominantly with two adjacent subunits of the channel, and Lys^{22} occludes the pore lumen like a cork in a bottle (Figure 4) (Kalman et al., 1998; Lanigan et al., 2002).

Guided by this knowledge, some 380 ShK analogs have been generated with the goal of developing a Kv1.3-specific inhibitor. Our early work focused on the full-length peptide as a significant decrease in potency was observed if we truncated ShK, made mono- and bis-disulfide analogs by replacing its disulfide bridges with the isostere surrogate alpha amino butyric acid, or stabilized its helical motifs with lactam rings (Lanigan et al., 2002; Pennington et al., 1999). When Lys^{22} was replaced with the shorter positively charged unnatural amino acid diaminopropionic acid (Dap), this analog, ShK-Dap^{22} (Kalman et al., 1998), blocked Kv1.3 with picomolar potency and exhibited >75-fold selectivity for Kv1.3 over Kv1.1 and other related channels (Table 2). Scientists at Amgen Inc., Thousand Oaks, California, have made a number of interesting ShK analogs (Sullivan et al., 2010). One of these, ShK-Q16K-PEG[20K], has ~1600-fold selectivity for Kv1.3 over Kv1.1 (Table 2). Another analog contains the heavy chain of an antibody attached to a single ShK-Q16K; this peptibody exhibits >1400-fold selectivity for Kv1.3 over Kv1.1 (Sullivan et al., 2010). Both these analogs may last longer in the circulation than ShK. Our analogs that are progressing

to the clinic have modifications at the N-terminus of the peptide (Table 2). ShK-170 contains a L-phosphotyrosine attached via a aminoethyloxyethyloxy-acetyl (Aeea) linker to the α-amino group of Arg^1 (Beeton et al., 2005). ShK-170 blocks Kv1.3 channels with an IC_{50} of 69 pM, and it is 100-fold selective for Kv1.3 over Kv1.1, 260-fold selective over Kv1.6, 280-fold selective over Kv3.2, 680-fold selective over Kv1.2, and >1000-fold selective over all other channels tested including KCa3.1 (Table 2). To stabilize the C-terminus of ShK-170 and improve its manufacturing aspects, we replaced the C-terminal carboxyl with an amide to minimize digestion by carboxypeptidases. The new analog, ShK-186 (Beeton et al., 2006), retains the selectivity and potency profile of ShK-170. Another analog, ShK-192, includes three stabilizing elements to minimize degradation: the N-terminal phosphotyrosine was replaced with the nonhydrolyzable phosphate mimetic *para*-phosphonophenylalanine (Ppa), Met^{21} was replaced with the isosteric homolog norleucine to avoid methionine oxidation, and the C-terminal was amidated (Pennington et al., 2009). ShK-192 blocks Kv1.3 with an IC_{50} of 140 pM and exhibits 30-fold selectivity over Kv3.2, 75-fold selectivity over Kv1.6 and 157-fold selectivity over Kv1.1 (Table 2).

4. ShK analogs are immunomodulatory

In vitro studies

ShK-186 inhibits Ca^{2+} signaling in human T_{EM} clones in a dose-dependent fashion with an IC_{50} ≈200 pM (Beeton et al., 2006). ShK-186 is significantly more effective in suppressing IL-2 and IFN-γ production by human $CCR7^-$ T_{EM} cells than $CCR7^+$ naïve/T_{CM} cells, but it is less effective in suppressing the production of TNF-α and IL-4 by either subset (Figure 5) (Beeton et al., 2006). ShK-186 is ≈10-fold more effective in suppressing proliferation ([^{3}H]thymidine incorporation) by human $CCR7^-$ T_{EM} cells compared with $CCR7^+$ T cells (Figure 5) (Beeton et al., 2006). When these cell populations are activated for 48 h, rested, and restimulated, $CCR7^-$ T_{EM}-effectors cells remain exquisitely sensitive to ShK-186 inhibition (IC_{50} ≈ 100 pM), whereas $CCR7^+$ effector cells (naïve-effector, T_{CM}-effector) are resistant (Figure 6). This “escape” by activated $CCR7^+$ naïve/T_{CM} cells is due to up-regulation of KCa3.1 that provides the counterbalancing K^+ efflux in these cells in place of Kv1.3. A significant aspect of this finding is that Kv1.3 blockers, unlike current immunomodulatory therapies that broadly suppress the immune response, would selectively suppress $CCR7^-$ T cells (T_{EM}/T_{EM} – effectors) implicated in autoimmune diseases, but not $CCR7^+$ T cells that are major mediators of immune protection. In support of this therapeutic concept, ShK-186, preferentially suppresses disease-associated autoreactive $CCR7^-$ T_{EM} cells (myelin- or GAD65-specific T cells or synovial T cells from affected joints) of MS and RA patients, respectively, without affecting other T cell subsets from these patients (Beeton et al., 2006).

ShK analogs have similar effects on rat T cells. ShK-170 suppressed myelin antigen-triggered proliferation of the rat $CCR7^-$ T_{EM} cell line, PAS (IC_{50} = 0.08 nM), >100-fold more effectively than mitogen-induced proliferation of rat splenic T cells (IC_{50} = 100 nM) (Beeton et al., 2005). Proliferation of the PAS cell line was also inhibited by Amgen’s ShK-Q16K-PEG[20K] analog (IC_{50} = 0.170 nM) and their ShK-Q16K-peptibody (IC_{50} = 0.84 nM) (Sullivan et al., 2010).

Delayed-type hypersensitivity (DTH), an in vivo model for inflammation caused by skin-homing $CCR7^-$ T_{EM} cells

We used the DTH model to determine the *in vivo* immunomodulatory efficacy of ShK analogs. Lewis rats were immunized with ovalbumin and complete Freund’s adjuvant, and a week later, one ear of each rat was injected with ovalbumin and the other ear with saline. Within 24 h, the ovalbumin-injected ear was significantly swollen, red and inflamed

compared to the saline-injected ear. Once daily subcutaneous injections (in the flank) of ShK-170 (10 μg/kg), ShK-186 (10 or 100 μg/kg) or ShK-192 (1, 10, or 100 μg/kg) suppressed the DTH response compared to rats administered saline (Beeton et al., 2005; Matheu et al., 2008; Pennington et al., 2009). [Note that ShK-170 and ShK-186 are identical, except for the C-terminal carboxyl in 170 is replaced by an amide in 186].

Two-photon microscopy was then used to image skin-homing $CCR7^-$ T_{EM}-effectors during DTH and assess the action of ShK-186 (Matheu et al., 2008). Within 3 h of antigen-challenge, GFP-labeled ovalbumin-specific $CCR7^-$ T_{EM}-effectors were visible in ovalbumin-injected ears where they formed stable contacts with tissue antigen-presenting cells. These T_{EM}-effectors activated over the course of a day, enlarged and began crawling rapidly along collagen fibers. This behavior coincided with massive swelling of the ovalbumin-injected ear. The saline-injected ear did not swell up, and very few ovalbumin-specific T_{EM}-effectors were seen. Treatment with ShK-186 (100 μg/kg once daily by subcutaneous injection) inhibited the DTH response by rendering $CCR7^-$ T_{EM}-effectors immotile in the ear and preventing their activation and enlargement (Matheu et al., 2008). The same dosing regimen had no effect on the motility of $CCR7^+$ T cells in lymphoid tissue, and it did not affect the motility of bystander cells. Prolonged immobilization of $CCR7^-$ T_{EM}-effector cells in inflamed tissues due to Kv1.3 blockade might prevent these cells from receiving activation and survival signals, thus leading to T_{EM} senescence via cytokine deprivation or the 'death-by-neglect' mechanism. In support of this, Kv1.3 channel blockers (margatoxin and correolide) suppress DTH to tuberculin in mini-pigs, and 2–3 weeks following the cessation of treatment, DTH cannot be elicited by repeat challenge with tuberculin (Koo et al., 1999; Koo et al., 1997). This period of 'remission' by Kv1.3 blocker therapy may be the result of the death-by-neglect mechanism whereby tuberculin-specific skin-homing $CCR7^-$ T cells are immobilized and then deleted at the site of DTH. Note, Koo et al., attributed the remission following Kv1.3 blocker-therapy to cellular depletion of the thymus (Koo et al., 1999; Koo et al., 1997).

Experimental Autoimmune Encephalomyelitis (EAE) – a model for multiple sclerosis

Myelin-specific T cells in patients with MS are predominantly $CCR7^-$ T_{EM}-effector cells with elevated Kv1.3 expression (Beeton et al., 2006; Wulff et al., 2003). To test whether such cells might be disease-inducing, we generated rat myelin-specific $CCR7^-$ T_{EM}-effector cell lines and compared their ability to induce experimental autoimmune encephalomyelitis (EAE) following adoptive transfer to healthy rats. Cells that expressed high numbers of Kv1.3 channels induced severe adoptive EAE compared to cells with lower numbers of Kv1.3 channels (Beeton et al., 2005; Beeton et al., 2001). Furthermore, ShK-170 suppressed myelin antigen-triggered proliferation of these $Kv1.3^{high}$ $CCR7^-$ T_{EM}-effectors, and its daily administration (10 μg/kg/day subcutaneous injection) both prevented and effectively treated adoptive EAE (Beeton et al., 2005). In the same model, Amgen's ShK-Q16K-PEG[20K] analog prevented adoptive EAE in a dose-dependent manner when administered once daily by subcutaneous injection (Sullivan et al., 2010).

Most patients with MS exhibit a relapsing and remitting clinical course of disease. EAE with a similar relapsing-remitting pattern can be induced by immunizing Dark Agouti (DA) rats with autologous spinal cord in emulsion with complete Freund's adjuvant. This disease is termed chronic relapsing-remitting EAE (CR-EAE). T cells in the central nervous system of these rats are predominantly $CCR7^-$ T_{EM}/T_{EM}-effectors during the chronic relapsing-remitting phase of the disease (Matheu et al., 2008). ShK-186 administered by once-daily subcutaneous injections (100 μg/kg/day) from the start of symptoms ameliorated CR-EAE by decreasing inflammatory cell-infiltration into the central nervous system and by decreasing demyelination (Matheu et al., 2008). Over the last 4 years, we have repeated these studies multiple times. In figure 7, we have compiled our data and compared clinical

scores in rats with CR-EAE that were treated with once-daily subcutaneous injections of vehicle (n=91), ShK-186 (100 μg/kg/day, n =53), or ShK-192 (100 μg/kg/day, n =20;1 μg/kg/day, n=20). A repeated-measures two-way ANOVA statistical test shows that ShK-186 and ShK-192 significantly reduced severity of disease (cumulative $p<0.001$).

Pristane-induced arthritis – a model for rheumatoid arthritis and psoriatic arthritis

ShK-186 was evaluated in a third autoimmune disease model. DA rats injected with pristane oil develop arthritis within 7–10 days, which is believed to be similar to RA and psoriatic arthritis (Hultqvist et al., 2006). In saline-treated rats, disease severity worsened continuously with time. Significant periostitis, erosion, and deformity were visible in X-rays of the joints, and pathological evaluation revealed severe synovitis, inflammatory cell infiltrate, and cartilage ulceration. ShK-186, administered from the start of symptoms by once-daily subcutaneous injections (100 μg/kg/day), significantly reduced the number of affected joints, and the rats showed significant improvement in radiological and histopathological findings (Beeton et al., 2006).

Autoimmune glomerulonephritis

In a rat model of anti-glomerular basement membrane glomerulonephritis, the majority of $CD4^+$ T cells and some $CD8^+$ T cells in the kidney were $Kv1.3^{high}$ T_{EM} cells (Hyodo et al., 2010). Some macrophages in the kidney infiltrate also expressed Kv1.3. Rats treated with the Kv1.3 inhibitor Psora-4 showed less proteinuria and fewer crescentic glomeruli than rats administered vehicle (Hyodo et al., 2010). ShK-186 may therefore be useful in the treatment of autoimmune kidney disease.

Inflammatory disorders of the skin

In a rat model of contact dermatitis, $CD8^+$ T_{EM} cells predominated amongst T cells infiltrating the skin during the elicitation phase (Azam et al., 2007). PAP-1, a Kv1.3 inhibitor (Table 2) (Schmitz et al., 2005), suppressed this disease by inhibiting the infiltration of $CD8^+$ T_{EM} cells and by reducing the production of the inflammatory cytokines IFNγ, IL-2, and IL-17 (Azam et al., 2007). In studies on psoriasis, more $Kv1.3^+$ immune cells were found in skin from patients with psoriasis than in normal human skin (Gilhar et al., 2011). Grafting of human psoriatic skin on to beige-SCID mice produced a condition resembling psoriasis, and local injections of ShK ameliorated disease by significantly reducing the number of $Kv1.3^+$ infiltrating cells (Gilhar et al., 2011). Interestingly, clofazimine, a drug that treats pustular psoriasis in humans (Chuaprapaisilp and Piamphongsant, 1978; Nair and Shereef, 1991), has been shown to block Kv1.3 with specificity over closely related channels (Ren et al., 2008) (Table 2). Seven decades of clinical use has revealed clofazimine to be generally safe, although it causes reversible skin discoloration in many patients, and prolonged therapy with high concentrations of clofazimine results in the formation of drug crystals in tissues, leading to eye problems, splenic infarction, and, in one case, death (Craythorn et al., 1986; McDougall et al., 1980) (Parizhskaya et al., 2001) (Mathew et al., 2006). These reports highlight the promise of Kv1.3 blockers such as ShK-186 for the treatment of inflammatory skin disorders.

Experimental autoimmune diabetes mellitus – a model for T1DM

Rats of the BB/Wor strain begin developing experimental autoimmune diabetes mellitus at the age of 70 days, and by 110 days disease-incidence is close to 100%. Once-daily oral administration of PAP-1 (50 mg/kg) significantly delayed the onset of disease in rats and only 47% of the rats had developed disease by 110 days (Beeton et al., 2006). Disease amelioration was associated with reduced infiltration of pancreatic islets by T cells and macrophages, and decreased β-cell destruction. Although Kv1.3 inhibitors are reported to

increase glucose uptake in mouse adipocytes by stimulating GLUT4 translocation (Li et al., 2006; Xu et al., 2004), PAP-1, ShK or margatoxin did not increase basal or insulin-stimulated glucose uptake by isolated cultured rat adipocytes, and did not enhance production of the insulin-sensitizing adipocyte hormone adiponectin by these cells (Beeton et al., 2006), indicating that PAP-1's therapeutic activity is likely to be via immunomodulation rather than a metabolic effect. ShK-186 (100 μg/kg once daily) delayed the onset of diabetes in these rats by about 10 days (Wulff and Pennington, 2007), but did not decrease disease incidence (data not shown). Differences in pharmacokinetic properties might explain the difference in efficacy of PAP-1 and ShK-186 in this model. Pharmacokinetic studies show that PAP-1 (logP 4.03) concentrates in the pancreas (a lipophilic organ) when compared to blood, and this accumulation may contribute to its therapeutic effectiveness (Beeton et al., 2006). ShK-186, a peptide with a net basic charge is unlikely to concentrate in the pancreas.

Studies on $Kv1.3^{-/-}$ mice suggest that Kv1.3 blockers might be effective in treating type-2 diabetes mellitus and obesity (Xu et al., 2003). $Kv1.3^{-/-}$ mice are more insulin sensitive and gain less weight on a high-fat diet than wild-type littermates, and blockade of Kv1.3 with margatoxin, a peptide from scorpion venom, increases peripheral insulin sensitivity in wild-type C57BL mice, and in db/db and ob/ob mice with type 2 diabetes mellitus and obesity (Xu et al., 2003). One mechanism for these therapeutic effects is that genetic deletion of Kv1.3 or pharmacological blockade of the channel promotes the translocation of the glucose transporter to the plasma membrane in adipose tissue and skeletal muscle, thereby enhancing peripheral insulin sensitivity (Xu et al., 2004). However, a recent study performed by scientists at Pfizer concluded that Kv1.3 is not involved in the modulation of peripheral insulin sensitivity (Straub et al., 2011). These authors demonstrated that Kv1.3 was not expressed in human adipose or skeletal muscle from healthy individuals or patients with type-2 diabetes mellitus, Kv1.3 blockers (PAP-1 or MgTX) did not alter glucose uptake into human skeletal muscle cells or mouse adipocytes, administration of PAP-1 failed to improve insulin sensitivity in hyperglycemic ob/ob mice at free plasma PAP-1 concentrations that are specific for inhibition of Kv1.3, and insulin sensitivity was only increased when PAP-1 concentrations were sufficient to inhibit other Kv1 channels (Straub et al., 2011). In other studies, deletion of Kv1.3 in mice lacking the melanocortin-4 receptor ($MC4R^{-/-}$ / $Kv1.3^{-/-}$) caused them to live longer, have a lower bodyweight, and enjoy increased reproductive success compared to $MC4R^{-/-}$ mice (Tucker et al., 2008). These changes were attributed to decreased fat deposition, reduced fasting leptin levels, and enhanced dark-phase locomotor activity and mass-specific metabolism (Tucker et al., 2008).

Transplantation

Of the approximately 20 billion T cells in human skin, about 85% are skin-homing $CCR7^{-}$ T_{EM} cells (Clark, 2010), which are probably critical for the rejection of skin transplants. Kv1.3 blockers may therefore be effective in preventing the rejection of skin grafts. In support of this idea, clofazimine, an inhibitor of Kv1.3 channels, prevented the rejection of grafted skin in an animal model (Ren et al., 2008). Human foreskin was grafted onto Pfb-$Rag2^{-/-}$ mice that lack T, B and NK cells (Ren et al., 2008). After the graft had healed, 100×10^6 human peripheral blood lymphocytes from an unrelated donor were adoptively transferred into the same animals and rejection of the skin graft was monitored. The graft was rejected within 11 days in vehicle-treated mice, but mice treated for 10 days with clofazimine did not reject the graft for 35 days, 20 days after the cessation of treatment (Ren et al., 2008).

In a study on kidney transplantation, ShK (80 μg/kg three times daily s.c.) in combination with the KCa3.1 blocker TRAM-34 (120 mg/kg/day i.p.) was as effective as cyclosporine A (5 mg/kg/day s.c.) in reducing infiltration of a kidney graft (from Fisher to Lewis rats) by

mononuclear cells, $CD8^+$ T cells and macrophages (Grgic et al., 2009). In another study, ShK-186 (300 μg/kg/day twice daily s.c.) and TRAM-34 (20 mg/kg/day twice daily, i.p.) delayed by two days rejection of pancreatic islets from Lewis rats that were grafted under the kidney capsule of DA rats. In contrast, rats that received cyclosporine A (5 mg/kg s.c), an immunomodulator that affects both $CCR7^+$ and $CCR7^-$ effectors, did not reject the transplanted islets for 60 days, and after cessation of the drug, islets were rejected in 2 weeks (Figure 8). Animals that received cyclosporine A for 21 days followed by either vehicle or ShK-186 (100 μg/kg/day s.c.), rejected islets in 2 weeks indicating that ShK-186 alone does not prevent acute rejection. Chronic rejection is believed to be mediated by $CCR7^-$ T_{EM} cells, and should be prevented by Kv1.3 blockers. In fact, clofazimine has been reported to prevent chronic graft-versus-disease in humans following bone marrow transplantation (Lee et al., 1997).

5. Pre-clinical development of ShK-186

Manufacture and formulation of ShK-186

ShK-186 has been manufactured under full GMP regulations at up to the 30 g scale using standard Fmoc-tBu solid-phase synthesis methods. Synthesis at this scale demonstrates the robustness of the manufacturing process, and is adequate to support clinical development through the expected range of human doses (approximately 1 – 15 μg/kg/week). Disulfide bond formation is achieved by air oxidation or using a glutathione exchange reaction. The manufacturing process provides a consistently pure and potent peptide with dissociation constants as measured on the cloned Kv1.3 channel consistent with published reports. Formulation of ShK-186 takes advantage of the inherent high degree of stability and solubility of this polybasic peptide (Tudor et al., 1998). Ideal liquid formulations are composed of phosphate-buffered isotonic solutions with a pH optimum around 6.0. Small amounts of surfactants can be added to the formulation to enhance resistance to peptide aggregation under various stress conditions. The resulting formulations are resistant to aggregation, exposure to ultraviolet light and serial freeze-thaw cycles. In addition, and despite the presence of a single oxidizable methionine in the peptide (Figure 4), formulated ShK-186 demonstrates good stability under forced oxidation conditions (0.01% hydrogen peroxide) for several hours. The resulting formulated drug product demonstrates long-term stability as a frozen or liquid formulation and is readily appropriate for early clinical development of the drug. The longer-term commercial development of a subcutaneous formulation will take advantage of the drug's solubility and potency to permit the use of small dose volumes and autoinjectors or needle-free injection systems.

Pharmacodynamic assay to measure ShK-186's immunomodulatory effect *in vivo*

A critical feature of the development of new drugs with novel mechanisms of action is the coordinate development of pharmacodynamic assays to measure and relate drug activity with drug exposure *in vivo*. Antagonism of Kv1.3 provides a special challenge due to its highly restricted functional role in $CCR7^-$ T cells (T_{EM}/T_{EM}-effector) and the paucity of this T cell subset in the vascular compartment (only 5–15% of the total T cells). An early attempt to characterize the pharmacodynamic activity of Kv1.3-selective inhibitors involved the *ex vivo* stimulation (PMA plus ionomycin) of peripheral blood mononuclear cells from minipigs treated with the scorpion toxin margatoxin (Koo et al., 1997). Drug treatment suppressed [^{3}H]-thymidine incorporation (Koo et al., 1999; Koo et al., 1997). This work was later expanded by Amgen to demonstrate that *ex vivo* stimulation of whole blood from cynomolgus monkeys treated with ShK analogs resulted in reduced expression of IL-2, IFN-γ, and IL-17 (Sullivan et al., 2010). Our analysis of *ex vivo* stimulated human whole blood suggests that a direct effect on Kv1.3 channel blockade can be measured using stimulations that exclusively trigger calcium signaling. For example, thapsigargin, an inhibitor of the

SERCA pump, empties the ER Ca^{2+} store and triggers the activation of CRAC channels on the cell surface, resulting in Ca^{2+} influx into T cells. The ensuing calcium-signaling cascade stimulates cytokine production without up-regulating the KCa3.1 channel by $CCR7^{+}$ T cells and their escape from Kv1.3 blocker-inhibition. This permits the effect of ShK-186 to be measured over the entire T cell population. Figure 9 shows that ShK-186 suppressed thapsigargin-induced production of cytokines by T cells in whole blood at picomolar concentrations with the following potency sequence: IL-2 = Th1 (IFN-γ) > Th17 (IL-17) > Th2 (IL-4). In a similar assay, ShK-Q16K-PEG[20K] inhibited IL-2 (IC_{50}: 109 pM) and IFN-γ (IC_{50}: 240 pM) production by human T cells, and IL-17 production by cynomolgus monkey T cells (Sullivan et al., 2010). Th1 and Th17 cells are implicated in the pathophysiology of autoimmune diseases (Damsker et al., 2010; Hemdan et al., 2011; Miossec et al., 2009). These drugs have no apparent effect on IL-6 or TNF-α production using the same system.

Amgen used the *ex vivo* assay to monitor the immunomodulatory effect of their ShK-Q16K-PEG[20K] analog in cynomolgus monkeys selected for high numbers of $CD4^{+}$ $CCR7^{-}$ T_{EM} cells (Sullivan et al., 2010). Monkeys received four once-weekly subcutaneous injections of the analog at 0.5 mg/kg. IL-17 was profoundly suppressed, and this suppression lasted for 2 weeks after cessation of treatment.

Pharmacokinetic studies

ShK analogs are clearly immunomodulatory if administered once daily by subcutaneous injection. We used a patch-clamp bioassay to ascertain whether circulating levels of ShK analogs after subcutaneous injection were sufficient to inhibit T_{EM} cells. ShK-170 was detectable in serum 5 min after a single subcutaneous injection of 200 μg/kg, peak levels of 12 nM were reached in 30 min and the level then fell to a baseline of approximately 0.3 nM over the next 7 h (Beeton et al., 2005). The disappearance of ShK-170 from the blood could be fitted by a single exponential curve, and the circulating half-life was estimated to be ~50 min. After a 20-fold lower dose of ShK-170 (10 μg/kg), the peak serum concentration reached ≈500 pM within 30 min, and repeated once-daily administration of this dose resulted in steady-state levels of 0.3 nM (Beeton et al., 2005). This steady-state level suggests that the peptide accumulates in the body on repeated administration. The route of administration—subcutaneous or intravenous—did not alter the steady-state level, indicating that this depot is not the skin, but rather lies elsewhere. ShK-186 and ShK-192 are also cleared from the circulation with a half-life of 30–50 min, but sufficient amounts of these peptides to cause immune suppression of $CCR7^{-}$ T_{EM} cells (0.2 nM) can be detected in the serum even 2 days after subcutaneous injection (Pennington et al., 2009). These results suggest that the peptide undergoes rapid clearance from the circulatory compartment into peripheral compartment(s), and then returns to the circulation at a steady-state level of ~0.2–0.3 nM. Interestingly, ultrafiltration followed by RP-HPLC shows that ~90% of ShK-186 is bound within 15 min to proteins in serum from rats, cynomoglus and humans (Figure 10). Serum protein-bound ShK-186 may constitute a reservoir of drug, although there are likely to be other compartments in the body. These data are consistent with the behavior of other positively-charged peptide drugs, which demonstrate rapid distribution from the central compartment and large apparent volumes of distribution (Boswell et al., 2010). These effects are thought to be mediated by low-affinity charge interactions between positively-charged drugs and abundant negatively charged surfaces throughout the body (Boswell et al.; Omar et al., 1992). Studies with the D-diastereomer of ShK emphasize that renal clearance rather than proteolysis is the major determinant of elimination-half-life of ShK peptides (Beeton et al., 2008). More careful pharmacokinetic studies with LC-MS and/or ELISA methods, or with radiolabeled ShK-186, are required to further characterize the pharmacokinetic properties of the peptide.

Amgen conducted pharmacokinetic studies with ShK-Q16K-PEG[20K] by the intravenous and subcutaneous routes of administration in mice, rats, beagles, and cynomolgus monkeys at doses ranging from 0.2 – 2 mg/kg. Following a single injection of 2 mg/kg ShK-Q16K-PEG[20K] to rats, peak levels of ~1000 ng/ml were measured at 24 h and the level dropped to 1 ng/ml 7 days later (Sullivan et al., 2010). After a single subcutaneous injection of 0.5 mg/kg to cynomolgus monkeys, a peak level of ~1000 ng/ml was measured during the first 24 h and the level remained high (~100 ng/ml, ~ 25 nM) 10 days later, indicating that the circulating half-life of this analog is significantly longer in monkeys than rats. Similar results were obtained with beagle dogs.

Safety studies

We performed a number of non-GLP studies in rats to determine the relative safety of ShK analogs. To determine if ShK-186 compromised the protective immune response, we examined whether rats treated with the peptide could clear infections of rat-adapted influenza virus or *Chlamydia*, a common sexually transmitted disease. Dexamethasone, a steroid that broadly suppresses the immune response, was used as a positive control, and saline as a negative control. Rats treated with saline or ShK-186 (100 μg/kg/day) cleared influenza infection in 4 days and *Chlamydia* infection in 14 days, whereas clearance of these infections was significantly delayed in dexamethasone-treated rats (Matheu et al., 2008). The small molecule Kv1.3 blocker PAP-1 similarly did not delay the clearance of influenza virus (Matheu et al., 2008). Thus, ShK-186, at concentrations that are therapeutic in DTH, EAE and PIA, does not compromise the protective immune response against acute infectious agents.

ShK-170, ShK-186 and ShK-192 were not cytotoxic on a panel of mammalian cell lines, and were negative in the Ames test (Beeton et al., 2005; Pennington et al., 2009). These peptides exhibit 10,000-fold selectivity for Kv1.3 over the HERG (Kv11.1) channel (Table 2), which underlies many drug-induced cardiac arrhythmias, and ShK-170 (10 μg/kg/day) did not alter heart rate variability parameters in rats (Beeton et al., 2005). ShK-186 administered once daily for 28 days to female Lewis rats by subcutaneous injection (100 μg/kg or 500 μg/kg per day) did not perceptibly alter blood cell counts or serum chemistry parameters, and it did not cause any histopathological changes in several tissues (brain, heart, lung, liver, kidney, gastrointestinal tract, pancreas, adrenal glands, urinary bladder, uterus, ovaries, thymus, spleen, mesenteric lymph node and bone marrow) (Beeton et al., 2006). We did detect low titer anti-ShK-186 antibodies in these rats (Beeton et al., 2006), but it remains to be determined whether these antibodies are neutralizing or have the potential to reduce the long-term therapeutic effectiveness of the peptide. In a study performed on cynomolgus monkeys at Amgen, no anti-peptide antibodies were detected in the animals that received low or high doses of ShK-Q16K-PEG[20K], whereas animals that received an intermediate doses of (0.5 mg/kg) developed such antibodies (Sullivan et al., 2010).

Amgen has conducted pharmacokinetic and toxicological studies on a number of ShK analogs in rats, dogs and monkeys. Single intravenous doses were evaluated in rats between 0.04 and 5 mg/kg. Repeat dose studies in rats evaluated weekly or every-third-day dosing of 0.1 – 5.0 mg/kg by the subcutaneous route for up to two weeks duration. Intravenous administration ShK-Q16K-PEG[20K], over all doses and subcutaneous administration at ≥0.3 mg/kg produced a consistent pattern of lethargy, weight loss, cyanosis, and vascular collapse in rats, with mortality in several of the dosing groups (Sullivan et al., 2010). These effects were observed in all rat strains tested (single 5 mg/kg SC dose) but not in studies involving administration to dog (single 0.2 mg/kg IV or 0.5 – 2.0 mg/kg SC dose), mouse (single 0.2 mg/kg IV dose, 0.6 – 5.0 mg/kg/day SC for 14 days), or cynomolgus monkey (single 0.2 mg/kg IV dose, 0.7 mg/kg SC every-third-day for two weeks or 0.1– 2.0 mg/kg/week SC for two weeks (Sullivan et al., 2010). Telemetrized rats also showed a reduction in

mean arterial blood pressure and increased heart rate following a single 0.7 and 2.5 mg/kg SC injection (Sullivan et al., 2010). Clinical observations were coincident with a finding of elevated serum histamine, leading the investigators to speculate that the adverse observations were due to mast cell degranulation (Sullivan et al., 2010). Positively-charged drugs like ShK are known to mediate IgE-independent anaphylactoid reactions (Mathelier-Fusade, 2006). In support of this idea, high doses (micromolar concentrations) of ShK-Q16K-PEG[20K], the ShK-Q16K-peptibody and ShK-192 released histamine from rat peritoneal mast cells in culture as effectively as known degranulators (e.g. compound 48/80). Patch-clamp studies of rat peritoneal mast cells did not reveal a Kv1.3 current, and the current in these cells was not sensitive to ShK analogs. This suggested a non-channel-dependent mechanism. Interestingly, these analogs did not induce histamine release from human or mouse mast cells, suggesting that the effect was species-specific (Sullivan et al., 2010). Furthermore, cynomolgus monkeys that received 0.7 mg/kg of ShK-Q16K-PEG[20K] every third day for 2 weeks, or 2 mg/kg once weekly for 2 weeks, or 0.5 mg/kg once weekly for four weeks, gained weight normally, no electrocardiogram changes were observed, and macroscopic and microscopic pathology analysis was normal. Total serum exposure to the peptide was significantly higher in these animals (mean AUC value of 584,000 ng × h/ml value) than in the rat toxicology studies. Based upon these observations, it is unlikely that humans receiving ShK analogs will exhibit histamine-mediated responses, since human T cells are >10,000 times more sensitive to Kv1.3 blocker-inhibition by ShK compared to the off-target degranulating effect on mast cells.

6. Overview and future directions

Three ion channels—Kv1.3, KCa3.1, Stim/Orai—regulate calcium signaling during the activation process in lymphocytes. All three of these channels cluster at the immunological synapse, the narrow cleft formed between the antigen-presenting cell (e.g. dendritic cell or macrophage or class-switched memory B cell) and the T lymphocyte. Kv1.3 and KCa3.1 regulate the membrane potential of lymphocytes and allow efflux of positively-charged ions (K^+) to counterbalance the influx of Ca^{2+} through CRAC (Stim1/Ora1) channels. The contribution of Kv1.3 and KCa3.1 to this process varies according to their relative expression level in $CCR7^+$ and $CCR7^-$ T cells, or IgD^+ and IgD^- B cells. Following antigen stimulation, human $CCR7^+$ T cells and IgD^+ B cells up-regulate KCa3.1 channels within 24 h, which then provides the counterbalancing K^+ efflux to sustain calcium signaling. In contrast, antigen stimulation of human $CCR7^-$ cells and IgD^- B cells, the two lymphoid subsets implicated in autoimmune diseases, results in the up-regulation of Kv1.3. The sensitivity of these two subsets to Kv1.3 channel-blockade offers opportunities for subset-selective immunomodulation in autoimmune disorders and chronic rejection. Kv1.3 blockers have been shown to be effective in numerous animal models of autoimmune disease, and disease-associated autoreactive T cells in the blood and tissues of patients with MS, RA and T1DM are $Kv1.3^{high}$ $CCR7^-$ T_{EM}-effectors. A synthetic derivative of a sea anemone peptide, ShK-186, blocks Kv1.3 at low picomolar concentrations and shows a high degree of selectivity for Kv1.3 over other channels. ShK-186 attenuates calcium signaling in $CCR7^-$ T_{EM} cells, suppresses cytokine production, proliferation and migration of these cells, and is effective in ameliorating DTH, and reducing disease-severity in animal models of MS and RA. Large-scale manufacture of this peptide has been achieved, a pharmacodynamic method has been developed for assessing immunomodulation *in vivo* and pharmacokinetic studies are underway. We anticipate beginning phase 1 human clinical trials with ShK-186 in 2011. Amgen has made PEGylated analogs of ShK and a peptibody of ShK, but the development status of these molecules is not known.

Acknowledgments

The work was supported by grant numbers: NIH RO1 NS48252 (KGC), NIH 1R43AI085691 (SI, KGC), NIH RO1 GM076063 (HW), UC Discovery 445160 (KGC, SI), Iacocca Foundation 485160 (SI, JTL, KGC), and fellowship support from the National Health and Medical Research Council of Australia (RSN).

References

Agematsu K, Hokibara S, Nagumo H, Komiyama A. CD27: a memory B-cell marker. Immunol. Today. 2000; 21:204–206. [PubMed: 10782048]

Azam P, Sankaranarayanan A, Homerick D, Griffey S, Wulff H. Targeting effector memory T cells with the small molecule Kv1.3 blocker PAP-1 suppresses allergic contact dermatitis. J. Invest. Dermatol. 2007; 127:1419–1429. [PubMed: 17273162]

Beeton C, Pennington MW, Wulff H, Singh S, Nugent D, Crossley G, Khaytin I, Calabresi PA, Chen CY, Gutman GA, Chandy KG. Targeting effector memory T cells with a selective peptide inhibitor of Kv1.3 channels for therapy of autoimmune diseases. Mol. Pharmacol. 2005; 67:1369–1381. [PubMed: 15665253]

Beeton C, Smith BJ, Sabo JK, Crossley G, Nugent D, Khaytin I, Chi V, Chandy KG, Pennington MW, Norton RS. The D-diastereomer of ShK toxin selectively blocks voltage-gated K^+ channels and inhibits T lymphocyte proliferation. J. Biol. Chem. 2008; 283:988–997. [PubMed: 17984097]

Beeton C, Wulff H, Barbaria J, Clot-Faybesse O, Pennington M, Bernard D, Cahalan MD, Chandy KG, Beraud E. Selective Blockade of T lymphocyte K^+ channels ameliorates experimental autoimmune encephalomyelitis, a model for multiple sclerosis. Proc. Natl. Acad. Sci. USA. 2001; 98:13942–13947. [PubMed: 11717451]

Beeton C, Wulff H, Standifer NE, Azam P, Mullen KM, Pennington MW, Kolski-Andreaco A, Wei E, Grino A, Counts DR, Wang PH, Leehealey CJ, B SA, Sankaranarayanan A, Homerick D, Roeck WW, Tehranzadeh J, Stanhope KL, Zimin P, Havel PJ, Griffey S, Knaus HG, Nepom GT, Gutman GA, Calabresi PA, Chandy KG. Kv1.3 channels are a therapeutic target for T cell-mediated autoimmune diseases. Proc. Natl. Acad. Sci. USA. 2006; 103:17414–17419. [PubMed: 17088564]

Boswell CA, Tesar DB, Mukhyala K, Theil FP, Fielder PJ, Khawli LA. Effects of charge on antibody tissue distribution and pharmacokinetics. Bioconjug. Chem. 2010; 21:2153–2163. [PubMed: 21053952]

Cahalan MD, Chandy KG. The functional network of ion channels in T lymphocytes. Immunol. Rev. 2009; 231:59–87. [PubMed: 19754890]

Castaneda O, Harvey AL. Discovery and characterization of *Cnidarian* peptide toxins that affect neuronal potassium ion channels. Toxicon. 2009; 54:1119–1124. [PubMed: 19269305]

Castaneda O, Sotolongo V, Amor AM, Stocklin R, Anderson AJ, Harvey AL, Engstrom A, Wernstedt C, Karlsson E. Characterization of a potassium channel toxin from the Caribbean sea anemone *Stichodactyla helianthus*. Toxicon. 1995; 33:603–613. [PubMed: 7660365]

Chandy KG, Wulff H, Beeton C, Pennington M, Gutman GA, Cahalan MD. Potassium channels as targets for specific immunomodulation. Trends Pharmacol. Sci. 2004; 25:280–289. [PubMed: 15120495]

Chuaprapaisilp T, Piamphongsant T. Treatment of pustular psoriasis with clofazimine. Br. J. Dermatol. 1978; 99:303–305. [PubMed: 708598]

Clark RA. Skin-resident T cells: the ups and downs of on site immunity. J. Invest. Dermatol. 2010; 130:362–370. [PubMed: 19675575]

Corcione A, Casazza S, Ferretti E, Giunti D, Zappia E, Pistorio A, Gambini C, Mancardi GL, Uccelli A, Pistoia V. Recapitulation of B cell differentiation in the central nervous system of patients with multiple sclerosis. Proc. Natl. Acad. Sci. USA. 2004; 101:11064–11069. [PubMed: 15263096]

Cotton J, Crest M, Bouet F, Alessandri N, Gola M, Forest E, Karlsson E, Castaneda O, Harvey A, Vita C, Menez A. A potassium-channel toxin from the sea anemone *Bunodosoma granulifera* an inhibitor for Kv1 channels. Revision of the amino acid sequence, disulfide-bridge assignment, chemical synthesis, and biological activity. Eur. J. Biochem. 1997; 244:192–202. [PubMed: 9063464]

Craythorn JM, Swartz M, Creel DJ. Clofazimine-induced bull's-eye retinopathy. Retina. 1986; 6:50–52. [PubMed: 3704351]

Damsker JM, Hansen AM, Caspi RR. Th1 and Th17 cells: adversaries and collaborators. Ann. New York Acad. Sci. 2010; 1183:211–221. [PubMed: 20146717]

DeCoursey TE, Chandy KG, Gupta S, Cahalan MD. Voltage-gated K^+ channels in human T lymphocytes: a role in mitogenesis? Nature. 1984; 307:465–468. [PubMed: 6320007]

Dorner T, Lipsky PE. Correlation of circulating CD27high plasma cells and disease activity in systemic lupus erythematosus. Lupus. 2004; 13:283–289. [PubMed: 15230280]

Fasth AE, Cao D, van Vollenhoven R, Trollmo C, Malmstrom V. $CD28^{null}CD4^+$ T cells-characterization of an effector memory T-cell population in patients with rheumatoid arthritis. Scand. J. Immunol. 2004; 60:199–208. [PubMed: 15238090]

Fordyce CB, Jagasia R, Zhu X, Schlichter LC. Microglia Kv1.3 channels contribute to their ability to kill neurons. J. Neurosci. 2005; 25:7139–7149. [PubMed: 16079396]

Friedrich M, Krammig S, Henze M, Docke WD, Sterry W, Asadullah K. Flow cytometric characterization of lesional T cells in psoriasis: Intracellular cytokine and surface antigen expression indicates an activated, memory effector/type 1 immunophenotype. Arch. Dermatol. Res. 2000; 292:519–521. [PubMed: 11142774]

Gendeh GS, Chung MC, Jeyaseelan K. Genomic structure of a potassium channel toxin from Heteractis magnifica. FEBS Lett. 1997a; 418:183–188. [PubMed: 9414123]

Gendeh GS, Young LC, de Medeiros CL, Jeyaseelan K, Harvey AL, Chung MC. A new potassium channel toxin from the sea anemone Heteractis magnifica: isolation, cDNA cloning, and functional expression. Biochemistry. 1997b; 36:11461–11471. [PubMed: 9298966]

Ghanshani S, Wulff H, Miller MJ, Rohm H, Neben A, Gutman GA, Cahalan MD, Chandy KG. Up-regulation of the IKCa1 potassium channel during T-cell activation: Molecular mechanism and functional consequences. J. Biol. Chem. 2000; 275:37137–37149. [PubMed: 10961988]

Gilhar A, Bergman R, Assay B, Ullmann Y, Etzioni A. The beneficial effect of blocking Kv1.3 in the psoriasiform SCID mouse model. J. Invest. Dermatol. 2011; 131:118–124. [PubMed: 20739949]

Grgic I, Wulff H, Eichler I, Flothmann C, Kohler R, Hoyer J. Blockade of T-lymphocyte KCa3.1 and Kv1.3 channels as novel immunosuppression strategy to prevent kidney allograft rejection. Transplant. Proc. 2009; 41:2601–2606. [PubMed: 19715983]

Hansen A, Odendahl M, Reiter K, Jacobi AM, Feist E, Scholze J, Burmester GR, Lipsky PE, Dorner T. Diminished peripheral blood memory B cells and accumulation of memory B cells in the salivary glands of patients with Sjogren's syndrome. Arthritis Rheum. 2002; 46:2160–2171. [PubMed: 12209521]

Hemdan NY, Birkenmeier G, Wichmann G, Abu El-Saad AM, Krieger T, Conrad K, Sack U. Interleukin-17-producing T helper cells in autoimmunity. Autoimmun. Rev. 2011; 9:785–792. [PubMed: 20647062]

Honma T, Kawahata S, Ishida M, Nagai H, Nagashima Y, Shiomi K. Novel peptide toxins from the sea anemone *Stichodactyla haddoni*. Peptides. 2008; 29:536–544. [PubMed: 18243416]

Hultqvist M, Olofsson P, Gelderman KA, Holmberg J, Holmdahl R. A new arthritis therapy with oxidative burst inducers. PLoS Med. 2006; 3:e348. [PubMed: 16968121]

Hyodo T, Oda T, Kikuchi Y, Higashi K, Kushiyama T, Yamamoto K, Yamada M, Suzuki S, Hokari R, Kinoshita M, Seki S, Fujinaka H, Yamamoto T, Miura S, Kumagai H. Voltage-gated potassium channel Kv1.3 blocker as a potential treatment for rat anti-glomerular basement membrane glomerulonephritis. Am. J. Physiol. Renal Physiol. 2010:F1258–F1269. [PubMed: 20810612]

Jacobi AM, Odendahl M, Reiter K, Bruns A, Burmester GR, Radbruch A, Valet G, Lipsky PE, Dorner T. Correlation between circulating CD27high plasma cells and disease activity in patients with systemic lupus erythematosus. Arthritis Rheum. 2003; 48:1332–1342. [PubMed: 12746906]

Kalman K, Pennington MW, Lanigan MD, Nguyen A, Rauer H, Mahnir V, Paschetto K, Kem WR, Grissmer S, Gutman GA, Christian EP, Cahalan MD, Norton RS, Chandy KG. ShK-Dap22, a potent Kv1.3-specific immunosuppressive polypeptide. J. Biol. Chem. 1998; 273:32697–32707. [PubMed: 9830012]

Khanna R, Roy L, Zhu X, Schlichter LC. K^+ channels and the microglial respiratory burst. Am. J. Physiol. Cell. Physiol. 2001; 280:C796–C806. [PubMed: 11245596]

Koo GC, Blake JT, Shah K, Staruch MJ, Dumont F, Wunderler D, Sanchez M, McManus OB, Sirotina-Meisher A, Fischer P, Boltz RC, Goetz MA, Baker R, Bao J, Kayser F, Rupprecht KM, Parsons WH, Tong XC, Ita IE, Pivnichny J, Vincent S, Cunningham P, Hora D Jr, Feeney W, Kaczorowski G, et al. Correolide and derivatives are novel immunosuppressants blocking the lymphocyte Kv1.3 potassium channels. Cell. Immunol. 1999; 197:99–107. [PubMed: 10607427]

Koo GC, Blake JT, Talento A, Nguyen M, Lin S, Sirotina A, Shah K, Mulvany K, Hora D Jr, Cunningham P, Wunderler DL, McManus OB, Slaughter R, Bugianesi R, Felix J, Garcia M, Williamson J, Kaczorowski G, Sigal NH, Springer MS, Feeney W. Blockade of the voltage-gated potassium channel Kv1.3 inhibits immune responses *in vivo*. J. Immunol. 1997; 158:5120–5128. [PubMed: 9164927]

Lanigan MD, Kalman K, Lefievre Y, Pennington MW, Chandy KG, Norton RS. Mutating a critical lysine in ShK toxin alters its binding configuration in the pore-vestibule region of the voltage-gated potassium channel, Kv1.3. Biochemistry. 2002; 41:11963–11971. [PubMed: 12356296]

Lee SJ, Wegner SA, McGarigle CJ, Bierer BE, Antin JH. Treatment of chronic graft-versus-host disease with clofazimine. Blood. 1997; 89:2298–2302. [PubMed: 9116272]

Leyendeckers H, Voth E, Schicha H, Hunzelmann N, Banga P, Schmitz J. Frequent detection of thyroid peroxidase-specific IgG^+ memory B cells in blood of patients with autoimmune thyroid disease. Eur. J. Immunol. 2002; 32:3126–3132. [PubMed: 12385033]

Li Y, Wang P, Xu J, Desir GV. Voltage-gated potassium channel Kv1.3 regulates GLUT4 trafficking to the plasma membrane via a Ca^{2+}-dependent mechanism. Am. J. Physiol. Cell. Physiol. 2006; 290:C345–C351. [PubMed: 16403947]

Lioudyno MI, Kozak JA, Penna A, Safrina O, Zhang SL, Sen D, Roos J, Stauderman KA, Cahalan MD. Orai1 and STIM1 move to the immunological synapse and are up-regulated during T cell activation. Proc. Natl. Acad. Sci. USA. 2008; 105:2011–2016. [PubMed: 18250319]

Lovett-Racke AE, Trotter JL, Lauber J, Perrin PJ, June CH, Racke MK. Decreased dependence of myelin basic protein-reactive T cells on CD28-mediated costimulation in multiple sclerosis patients: a marker of activated/memory T cells. J. Clin. Invest. 1998; 101:725–730. [PubMed: 9466965]

Luik RM, Wang B, Prakriya M, Wu MM, Lewis RS. Oligomerization of STIM1 couples ER calcium depletion to CRAC channel activation. Nature. 2008; 454:538–542. [PubMed: 18596693]

Mathelier-Fusade P. Drug-induced urticarias. Clin Rev Allergy Immunol. 2006; 30:19–23. [PubMed: 16461991]

Matheu MP, Beeton C, Garcia A, Chi V, Rangaraju S, Safrina O, Monaghan K, Uemura MI, Li D, Pal S, de la Maza LM, Monuki E, Flugel A, Pennington MW, Parker I, Chandy KG, Cahalan MD. Imaging of effector memory T cells during a delayed-type hypersensitivity reaction and suppression by Kv1.3 channel block. Immunity. 2008; 29:602–614. [PubMed: 18835197]

Mathew BS, Pulimood AB, Prasanna CG, Ramakrishna BS, Chandy SJ. Clofazimine induced enteropathy--a case highlighting the importance of drug induced disease in differential diagnosis. Trop. Gastroenterol. 2006; 27:87–88. [PubMed: 17089619]

Matteson DR, Deutsch C. K channels in T lymphocytes: a patch clamp study using monoclonal antibody adhesion. Nature. 1984; 307:468–471. [PubMed: 6320008]

McDougall AC, Horsfall WR, Hede JE, Chaplin AJ. Splenic infarction and tissue accumulation of crystals associated with the use of clofazimine (Lamprene; B663) in the treatment of pyoderma gangrenosum. Br. J. Dermatol. 1980; 102:227–230. [PubMed: 7387877]

Miossec P, Korn T, Kuchroo VK. Interleukin-17 and type 17 helper T cells. N. Engl. J. Med. 2009; 361:888–898. [PubMed: 19710487]

Miyazaki Y, Iwabuchi K, Kikuchi S, Fukazawa T, Niino M, Hirotani M, Sasaki H, Onoe K. Expansion of CD4+CD28− T cells producing high levels of interferon-{gamma} in peripheral blood of patients with multiple sclerosis. Mult. Scler. 2008; 14:1044–1055. [PubMed: 18573819]

Mouhat S, Visan V, Ananthakrishnan S, Wulff H, Andreotti N, Grissmer S, Darbon H, De Waard M, Sabatier JM. K^+ channel types targeted by synthetic OSK1, a toxin from *Orthochirus scrobiculosus* scorpion venom. Biochem. J. 2005; 385:95–104. [PubMed: 15588251]

Mullen KM, Rozycka M, Rus H, Hu L, Cudrici C, Zafranskaia E, Pennington MW, Johns DC, Judge SI, Calabresi PA. Potassium channels Kv1.3 and Kv1.5 are expressed on blood-derived dendritic cells in the central nervous system. Ann. Neurol. 2006; 60:118–127. [PubMed: 16729292]

Nagumo H, Agematsu K, Kobayashi N, Shinozaki K, Hokibara S, Nagase H, Takamoto M, Yasui K, Sugane K, Komiyama A. The different process of class switching and somatic hypermutation; a novel analysis by CD27(−) naive B cells. Blood. 2002; 99:567–575. [PubMed: 11781240]

Nair LV, Shereef PH. Successful treatment of generalized pustular psoriasis with clofazimine. Int. J. Dermatol. 1991; 30:151. [PubMed: 2001910]

Nicolaou SA, Neumeier L, Peng Y, Devor DC, Conforti L. The Ca^{2+}-activated K^+ channel KCa3.1 compartmentalizes in the immunological synapse of human T lymphocytes. Am. J. Physiol. Cell. Physiol. 2007:C1431–C1439. [PubMed: 17151145]

Norton RS, Pennington MW, Wulff H. Potassium channel blockade by the sea anemone toxin ShK for the treatment of multiple sclerosis and other autoimmune diseases. Curr. Med. Chem. 2004; 11:3041–3052. [PubMed: 15578998]

Omar BA, Flores SC, McCord JM. Superoxide dismutase: pharmacological developments and applications. Adv. Pharmacol. 1992; 23:109–161. [PubMed: 1531762]

Panyi G, Vamosi G, Bacso Z, Bagdany M, Bodnar A, Varga Z, Gaspar R, Matyus L, Damjanovich S. Kv1.3 potassium channels are localized in the immunological synapse formed between cytotoxic and target cells. Proc. Natl. Acad. Sci. USA. 2004; 101:1285–1290. [PubMed: 14745040]

Parizhskaya M, Youssef NN, Di Lorenzo C, Goyal RK. Clofazimine enteropathy in a pediatric bone marrow transplant recipient. J. Pediatr. 2001; 138:574–576. [PubMed: 11295724]

Park CY, Hoover PJ, Mullins FM, Bachhawat P, Covington ED, Raunser S, Walz T, Garcia KC, Dolmetsch RE, Lewis RS. STIM1 clusters and activates CRAC channels via direct binding of a cytosolic domain to Orai1. Cell. 2009; 136:876–890. [PubMed: 19249086]

Penna A, Demuro A, Yeromin AV, Zhang SL, Safrina O, Parker I, Cahalan MD. The CRAC channel consists of a tetramer formed by Stim-induced dimerization of Orai dimers. Nature. 2008; 456:116–120. [PubMed: 18820677]

Pennington M, Byrnes M, Zaydenberg I, Khaytin I, de Chastonay J, Krafte D, Hill R, Mahnir V, Volberg W, Gorczyca W, Kem W. Chemical synthesis and characterization of ShK toxin: a potent potassium channel inhibitor from a sea anemone. Int. J. Pept. Protein Res. 1995; 346:354–358. [PubMed: 8567178]

Pennington M, Lanigan M, Kalman K, Mahnir V, Rauer H, McVaugh C, Behm D, Donaldson D, Chandy K, Kem W, Norton R. Role of disulfide bonds in the structure and potassium channel blocking activity of ShK toxin. Biochemistry. 1999; 38:14549–14558. [PubMed: 10545177]

Pennington M, Mahnir V, Khaytin I, Zaydenberg I, Byrnes M, Kem W. An essential binding surface for ShK toxin interaction with rat brain potassium channels. Biochemistry. 1996; 35:16407–16411. [PubMed: 8987971]

Pennington MW, Beeton C, Galea CA, Smith BJ, Chi V, Monaghan KP, Garcia A, Rangaraju S, Giuffrida A, Plank D, Crossley G, Nugent D, Khaytin I, Lefievre Y, Peshenko I, Dixon C, Chauhan S, Orzel A, Inoue T, Hu X, Moore RV, Norton RS, Chandy KG. Engineering a stable and selective peptide blocker of the Kv1.3 channel in T lymphocytes. Mol. Pharmacol. 2009; 75:762–773. [PubMed: 19122005]

Pereira LE, Villinger F, Wulff H, Sankaranarayanan A, Raman G, Ansari AA. Pharmacokinetics, toxicity, and functional studies of the selective Kv1.3 channel blocker 5-(4-phenoxybutoxy)psoralen in rhesus macaques. Exp. Biol. Med. (Maywood). 2007; 232:1338–1354. [PubMed: 17959847]

Pohl J, Hubalek F, Byrnes ME, Nielsen KR, Woods A, Pennington MW. Assignment of the three disulfide bonds in ShK toxin: A potent potassium channel inhibitor from the sea anemone Stichodactyla helianthus. Lett. In Peptide Sci. 1995; 1:291–297.

Rauer H, Pennington M, Cahalan M, Chandy KG. Structural conservation of the pores of calcium-activated and voltage-gated potassium channels determined by a sea anemone toxin. J. Biol. Chem. 1999; 274:21885–21892. [PubMed: 10419508]

Ren YR, Pan F, Parvez S, Fleig A, Chong CR, Xu J, Dang Y, Zhang J, Jiang H, Penner R, Liu JO. Clofazimine inhibits human Kv1.3 potassium channel by perturbing calcium oscillation in T lymphocytes. PLoS ONE. 2008; 3:e4009. [PubMed: 19104661]

Rus H, Pardo CA, Hu L, Darrah E, Cudrici C, Niculescu T, Niculescu F, Mullen KM, Allie R, Guo L, Wulff H, Beeton C, Judge SI, Kerr DA, Knaus HG, Chandy KG, Calabresi PA. The voltage-gated potassium channel Kv1.3 is highly expressed on inflammatory infiltrates in multiple sclerosis brain. Proc. Natl. Acad. Sci. USA. 2005; 102:11094–11099. [PubMed: 16043714]

Sallusto F, Lenig D, Forster R, Lipp M, Lanzavecchia A. Two subsets of memory T lymphocytes with distinct homing potentials and effector functions. Nature. 1999; 401:708–712. [PubMed: 10537110]

Schlichter L, Sidell N, Hagiwara S. Potassium channels mediate killing by human natural killer cells. Proc. Natl. Acad. Sci. USA. 1986; 83:451–455. [PubMed: 2417243]

Schmitz A, Sankaranarayanan A, Azam P, Schmidt-Lassen K, Homerick D, Hansel W, Wulff H. Design of PAP-1, a selective small molecule Kv1.3 blocker, for the suppression of effector memory T cells in autoimmune diseases. Mol. Pharmacol. 2005; 68:1254–1270. [PubMed: 16099841]

Shiomi K. Novel peptide toxins recently isolated from sea anemones. Toxicon. 2009; 54:1112–1118. [PubMed: 19269303]

Sidell N, Schlichter LC, Wright SC, Hagiwara S, Golub SH. Potassium channels in human NK cells are involved in discrete stages of the killing process. J. Immunol. 1986; 137:1650–1658. [PubMed: 2427578]

Straub SV, Perez SM, Tan B, Coughlan KA, Trebino CE, Cosgrove P, Buxton JM, Kreeger JM, Jackson VM. Pharmacological inhibition of Kv1.3 fails to modulate insulin sensitivity in diabetic mice or human insulin-sensitive tissues. Am. J. Physiol. Endocrinol. Metab. 2011 Epub date 2011/05/19.

Sullivan, JK.; Miranda, LP.; Gegg, CV.; Hu, S.; Belouski, EJ.; Murray, JK.; Nguyen, H.; Walker, KW.; Arora, T.; Jacobsen, FW.; Li, Y.; Boone, TC. Selective and potent peptide inhibitors of Kv1.3. WO 2010/108154A2. 2010. p. 288

Tucker K, Overton JM, Fadool DA. Kv1.3 gene-targeted deletion alters longevity and reduces adiposity by increasing locomotion and metabolism in melanocortin-4 receptor-null mice. Int. J. Obes. (Lond.). 2008; 32:1222–1232. [PubMed: 18542083]

Tudor JE, Pallaghy PK, Pennington MW, Norton RS. Solution structure of ShK toxin, a novel potassium channel inhibitor from a sea anemone. Nat. Struct. Biol. 1996; 3:317–320. [PubMed: 8599755]

Tudor JE, Pennington MW, Norton RS. Ionisation behaviour and solution properties of the potassium-channel blocker ShK toxin. Eur. J. Biochem. 1998; 251:133–141. [PubMed: 9492277]

Vennekamp J, Wulff H, Beeton C, Calabresi PA, Grissmer S, Hansel W, Chandy KG. Kv1.3-blocking 5-phenylalkoxypsoralens: a new class of immunomodulators. Mol. Pharmacol. 2004; 65:1364–1374. [PubMed: 15155830]

Viglietta V, Kent SC, Orban T, Hafler DA. GAD65-reactive T cells are activated in patients with autoimmune type 1a diabetes. J. Clin. Invest. 2002; 109:895–903. [PubMed: 11927616]

Vissers WH, Arndtz CH, Muys L, Van Erp PE, de Jong EM, van de Kerkhof PC. Memory effector ($CD45RO^+$) and cytotoxic ($CD8^+$) T cells appear early in the margin zone of spreading psoriatic lesions in contrast to cells expressing natural killer receptors, which appear late. Br. J. Dermatol. 2004; 150:852–859. [PubMed: 15149496]

Wulff H, Calabresi PA, Allie R, Yun S, Pennington M, Beeton C, Chandy KG. The voltage-gated Kv1.3 K^+ channel in effector memory T cells as new target for MS. J. Clin. Invest. 2003; 111:1703–1713. [PubMed: 12782673]

Wulff H, Knaus HG, Pennington M, Chandy KG. K^+ channel expression during B-cell differentiation: implications for immunomodulation and autoimmunity. J. Immunol. 2004; 173:776–786. [PubMed: 15240664]

Wulff H, Pennington M. Targeting effector memory T-cells with Kv1.3 blockers. Curr. Opin. Drug Discov. Devel. 2007; 10:438–445.

Xu J, Koni PA, Wang P, Li G, Kaczmarek L, Wu Y, Li Y, Flavell RA, Desir GV. The voltage-gated potassium channel Kv1.3 regulates energy homeostasis and body weight. Human Mol. Gen. 2003; 12:551–559.

Xu J, Wang P, Li Y, Li G, Kaczmarek LK, Wu Y, Koni PA, Flavell RA, Desir GV. The voltage-gated potassium channel Kv1.3 regulates peripheral insulin sensitivity. Proc. Natl. Acad. Sci. USA. 2004; 101:3112–3117. [PubMed: 14981264]

Yamaguchi Y, Hasegawa Y, Honma T, Nagashima Y, Shiomi K. Screening and cDNA cloning of Kv1 potassium channel toxins in sea anemones. Mar. Drugs. 2011; 8:2893–2905. [PubMed: 21339955]

Zsiros E, Kis-Toth K, Hajdu P, Gaspar R, Bielanska J, Felipe A, Rajnavolgyi E, Panyi G. Developmental switch of the expression of ion channels in human dendritic cells. J. Immunol. 2009; 183:4483–4492. [PubMed: 19748986]

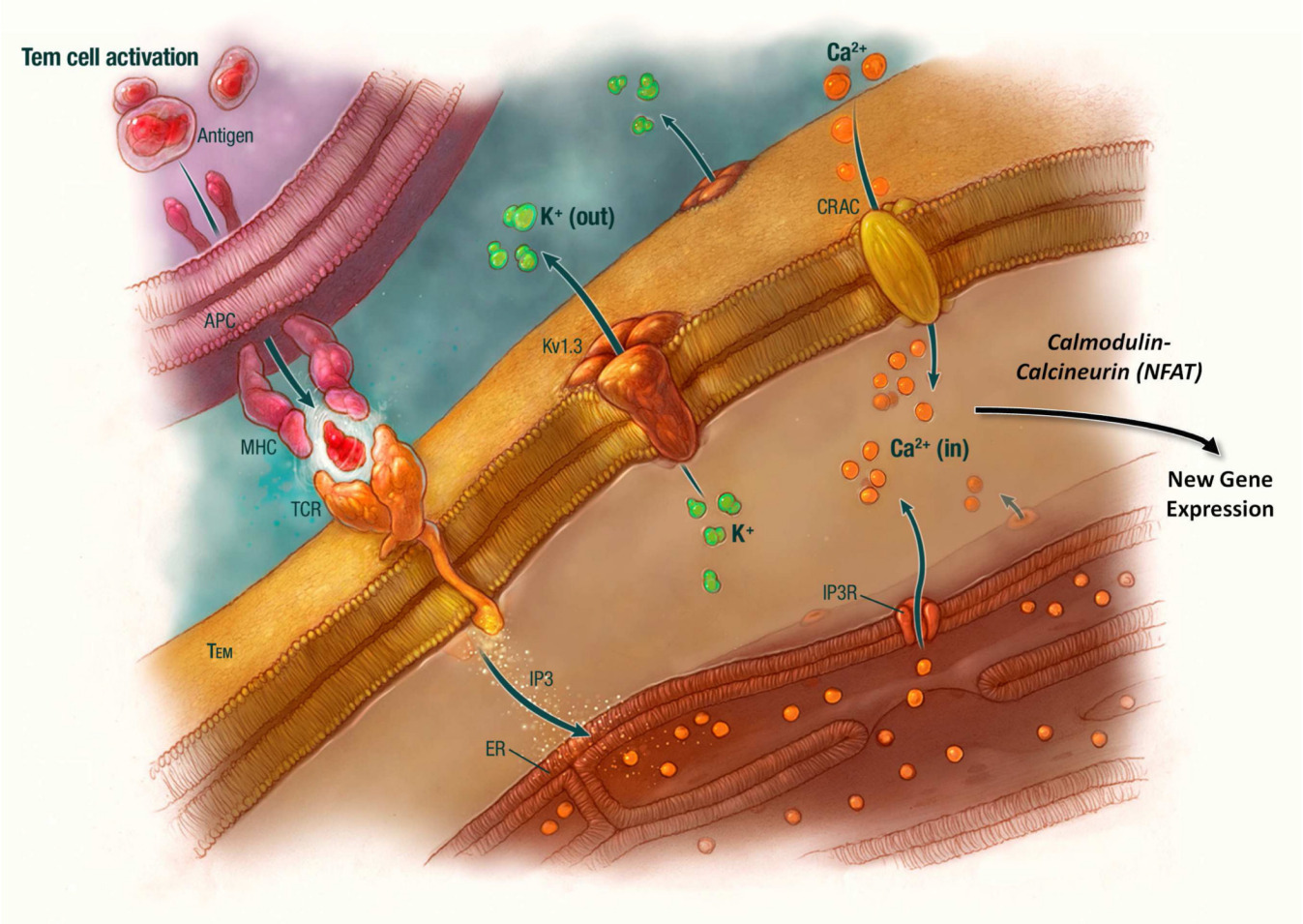

Figure 1. Kv1.3 channels provide the counterbalancing K^+ efflux for Ca^{2+} entry into CCR7$^-$ T_{EM}-effector cells

Top left of the figure is an antigen-presenting cell (APC), which processes and presents antigen via MHC to the T-cell receptor (TCR) on a T_{EM} cell. A signaling cascade is initiated involving the production of IP3 and the release of calcium from internal stores via the IP_3-triggered IP_3 receptor leading to an increase in cytosolic calcium to about 250 nM. Emptying of the stores causes calcium to enter T cells via CRAC channels, resulting in the calcium level rising to about 1 μM. The calcium signaling cascade initiates new gene expression via the calmodulin-calcineurin-NFAT pathway.

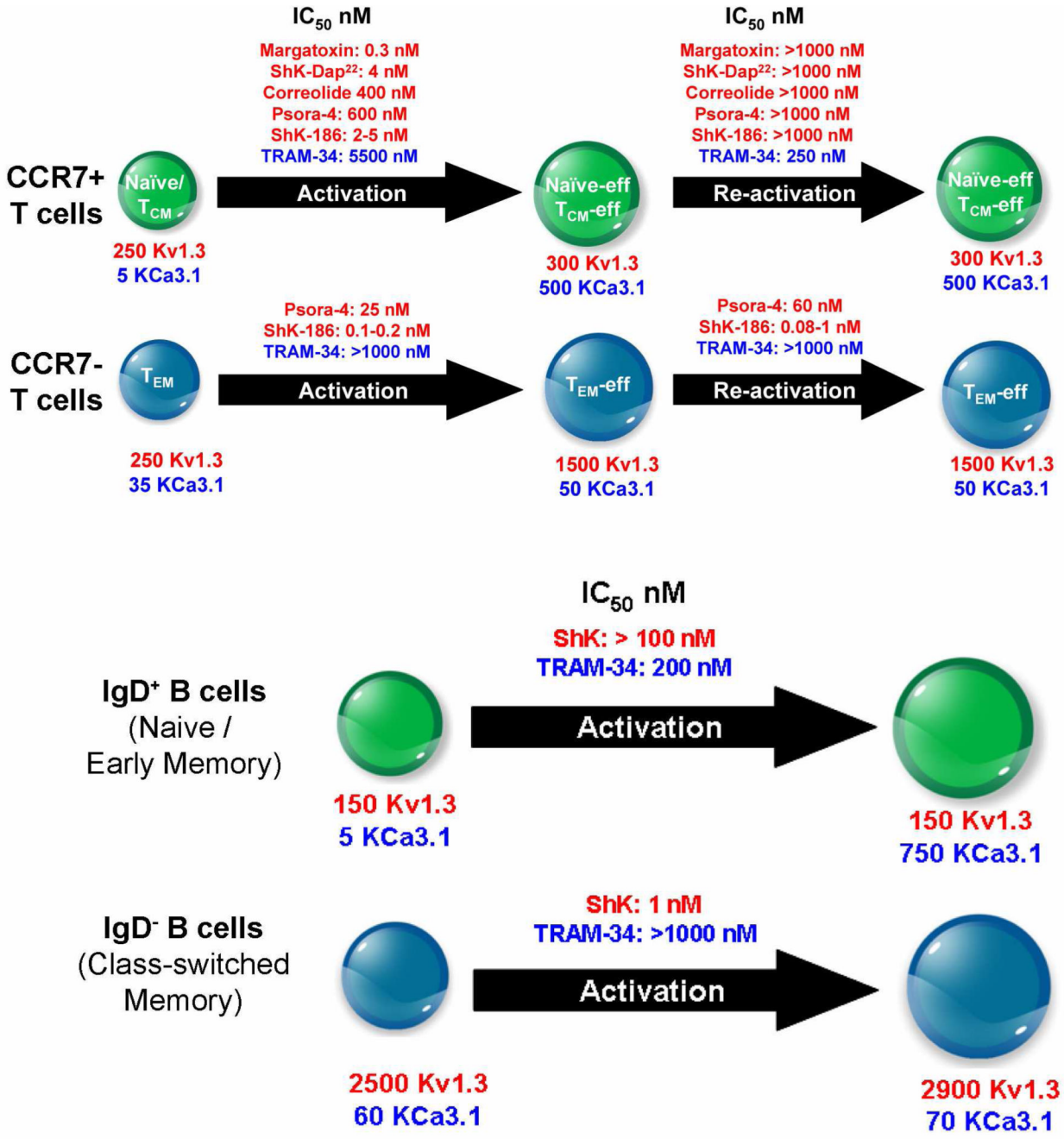

Figure 2. K^+ Channel-expression patterns in human T and B cells, and sensitivity to block by Kv1.3 and KCa3.1 blockers

A, Numbers of Kv1.3 and KCa3.1 channels per cell in $CCR7^+$ naïve or $CCR7^+T_{CM}$ cells as they activate into naïve-effectors or T_{CM}-effectors, respectively, and in $CCR7^-$ T_{EM} cells when the activate into T_{EM}-effectors. Activation was with anti-CD3 antibody. In some experiments, the cells were washed, rested, reactivated with anti-CD3 antibody. The effect of Kv1.3-specific and KCa3.1-specific blockers on proliferation ($[^3H]$-thymidine incorporation) during activation is shown. **B,** Kv1.3 and KCa3.1 channels/cell in IgD^+ B cells (naïve or early memory) and IgD^- B cells (class-switched memory) following activation, and the effect of K^+ channel inhibitors.

A

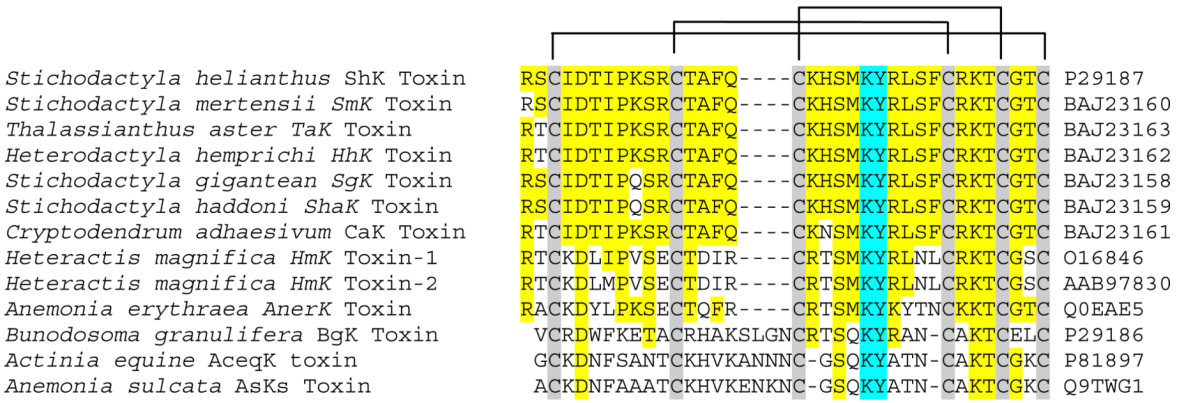

B

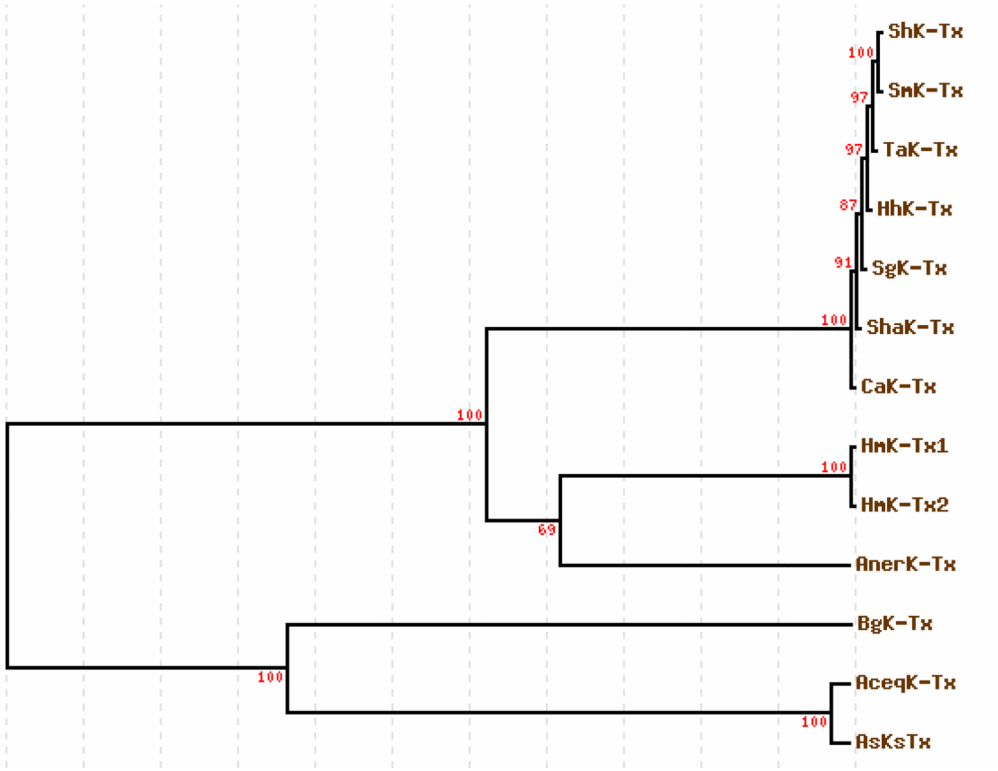

Figure 3.

A, Alignment of ShK and related sea anemone toxins: The six cysteines are in grey and the disulfide pairing is shown. Lys[22] and Tyr[23] are highlighted in blue. Lys[22] occupies the lumen of the Kv1.3 channel pore. GenBank Accession numbers are listed next to each sequence. Many of these sea anemone toxin sequences have been characterized for K^+ channel-blocking activity (Castaneda et al., 1995; Cotton et al., 1997; Gendeh et al., 1997a; Gendeh et al., 1997b; Honma et al., 2008; Shiomi, 2009) (Yamaguchi et al., 2011). **B, A phylogenetic tree based on the multiple sequence alignment and generated with the PHYLIP program** (http://www.genebee.msu.su/genebee.html): ShK (ShK-Tx) and toxins

from six other sea anemones (S. *mertensii* [SmK-Tx], S. *haddoni* [ShaK-Tx], S. *gigantean* [SgK-Tx], *T. aster* [TaK-Tx], *C. adhaesivum* [CaK-Tx], *H. magnifica* [HhK-Tx]) have the same number of residues as ShK, share remarkable sequence similarity, and cluster in one sub-group. Two toxins from *Heteractis magnifica* (HmK-Tx1, HmK-Tx2) and the toxin from *Anemonia erythraea* (AnerK-Tx) have the same number of residues as ShK, and comprise a closely-related but distinct cluster. Toxins from three other sea anemones (*B. granulifera* [BgK-Tx], *A. equine* [AceqK-Tx], *A. sulcata* [AsKs-Tx]) exemplified by the BgK toxin contain four extra residues between cysteines 3 and 4, and constitute a distinct, yet ShK-related group.

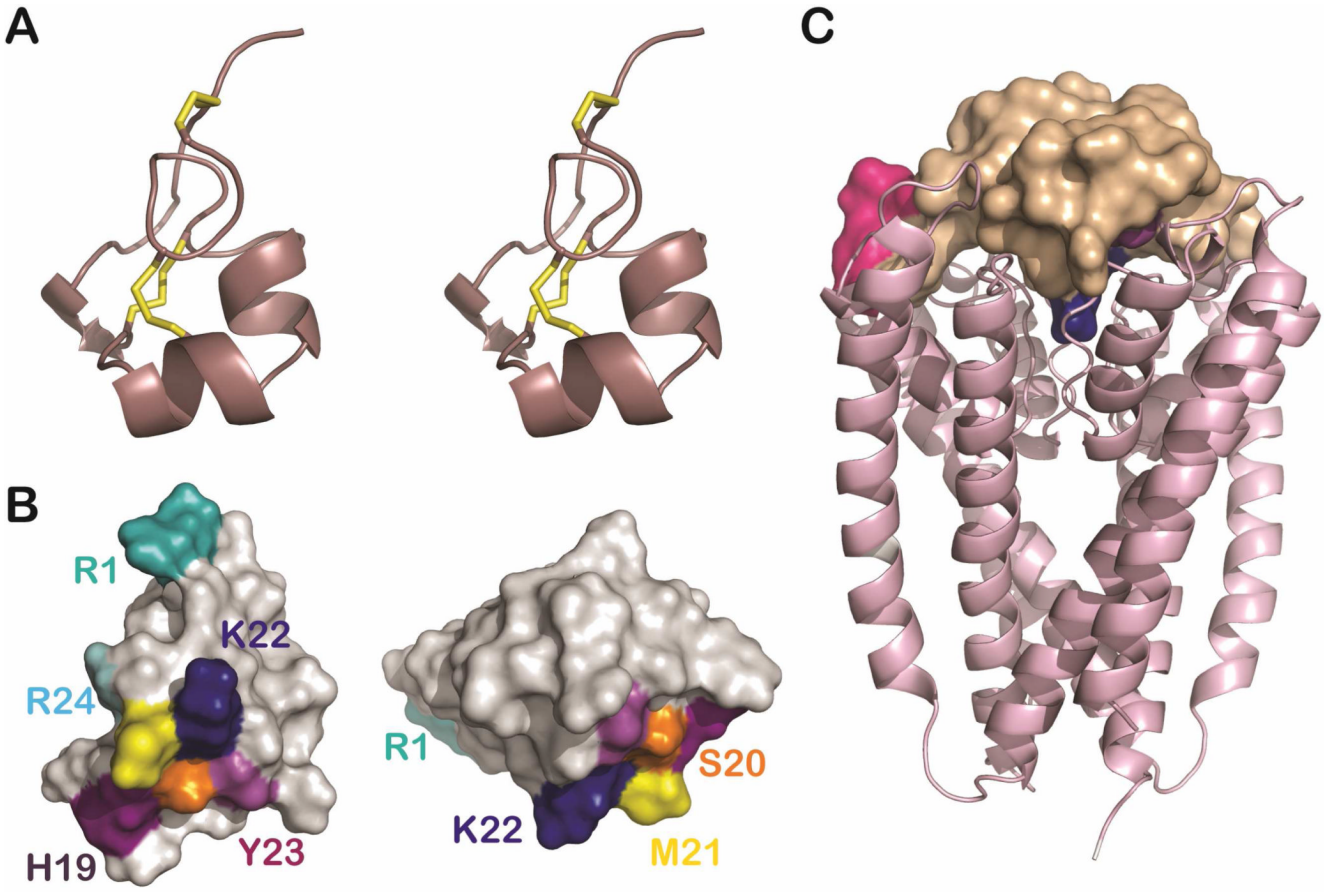

Figure 4.

A, Stereo view of the closest-to-average structure of ShK in solution (PDB id 1ROO) (Tudor et al., 1996). The three disulfide bridges (Cys^{3}-Cys^{35}, Cys^{12}-Cys^{28}, and Cys^{17} Cys^{32}) are shown in yellow. *B,* Surface views of ShK with key residues coloured as follows: Lys22 blue, Tyr23 magenta, His19 deep purple, Ser^{20} orange and Arg^{24} cyan. Met^{21}, which is susceptible to oxidation, is colored yellow and Arg^{1} is colored teal as a reference point. In the right hand view, Arg^{24} is not visible and Arg^{1} lies at the far left of the structure; this orientation is similar to that of ShK-192 in part C. ***C,*** Structure of ShK-192 docked with a model of the pore-vestibule region of Kv1.3 (Pennington et al., 2009). Kv1.3 is shown in a ribbon representation, while ShK-192 is shown as a molecular surface, with all residues colored wheat except Lys^{22}, which is colored blue, Tyr^{23} magenta and the N-terminal extension pink.

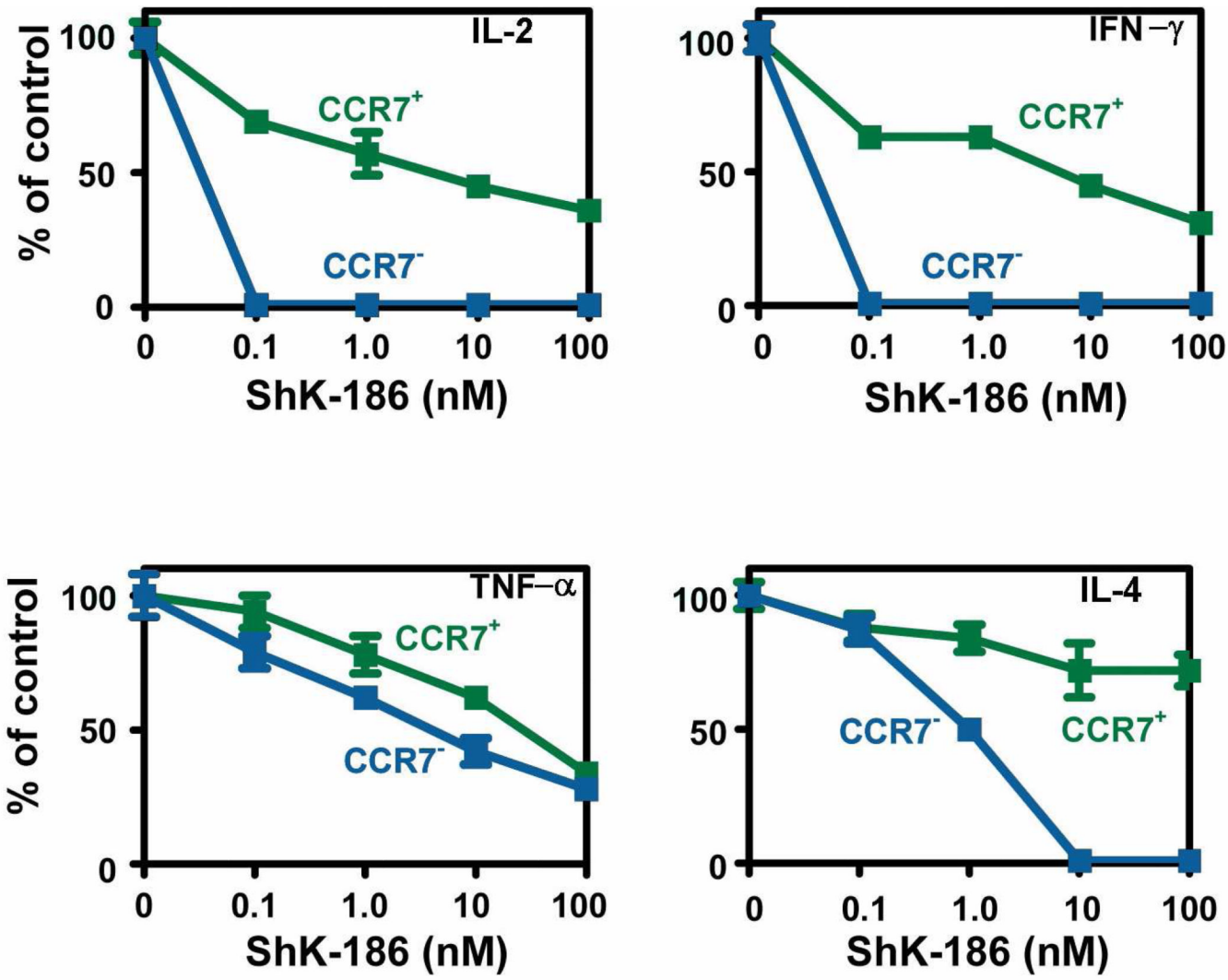

Figure 5. Effect of ShK-186 on cytokine production by human T cell subsets activated with anti-CD3 antibody

Adapted from (Beeton et al., 2006).

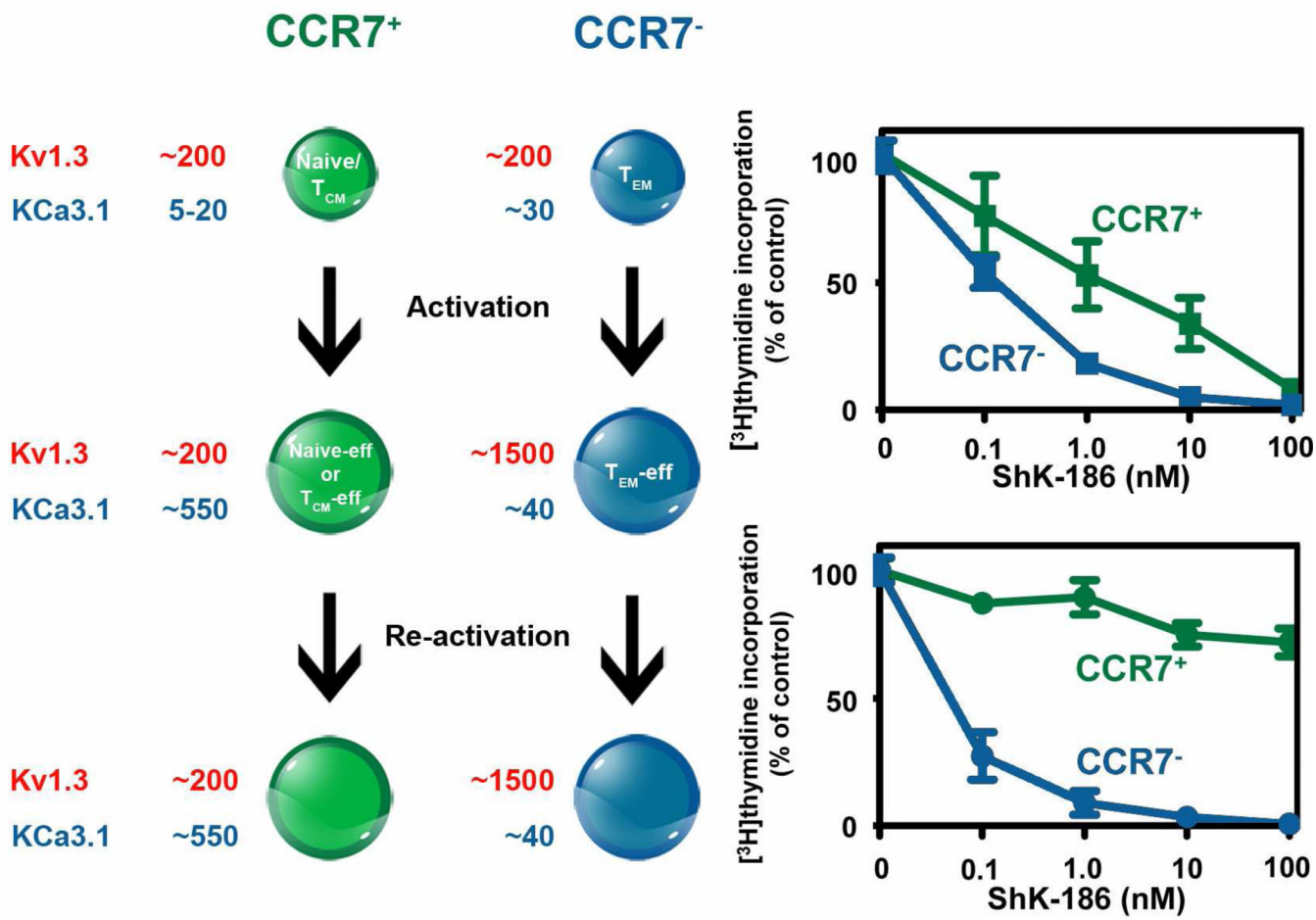

Figure 6. Effect of ShK-186 on proliferation ([^{3}H]-thymidine incorporation) by human T cell subsets activated with anti-CD3 antibody

(adapted from (Beeton et al., 2006). The K^+ channel expression patterns of $CCR7^+$ and $CCR7^-$ T cells are shown when they are at rest, when activated into effectors, and when reactivated. The pharmacological sensitivity to ShK-186 depends on the channel expression pattern. ShK-186 suppresses $CCR7^+$ naïve/T_{CM} cells with an IC_{50} value of 2–5 nM, whereas $CCR7^-$ T_{EM} cells are suppressed with an IC_{50} value = 0.1–0.2 nM. The roughly 10-fold lower sensitivity of $CCR7^+$ T cells is because they up-regulate KCa3.1 during the activation process. When $CCR7^+$ effectors are reactivated, they are insensitive to ShK-186 because their membrane potential is dominated by ShK-186-resistant KCa3.1 channels, whereas $CCR7^-$ effectors are suppressed with an IC_{50} = 0.08–0.1 nM. Similar results are obtained with rat T cells. ShK-170 suppresses mitogen-induced proliferation of rat splenic T cells with an IC_{50} = 100 nM, whereas it suppresses antigen-triggered proliferation of the rat $CCR7^-$ T_{EM} cell line, PAS, with an IC_{50} = 0.08 nM.

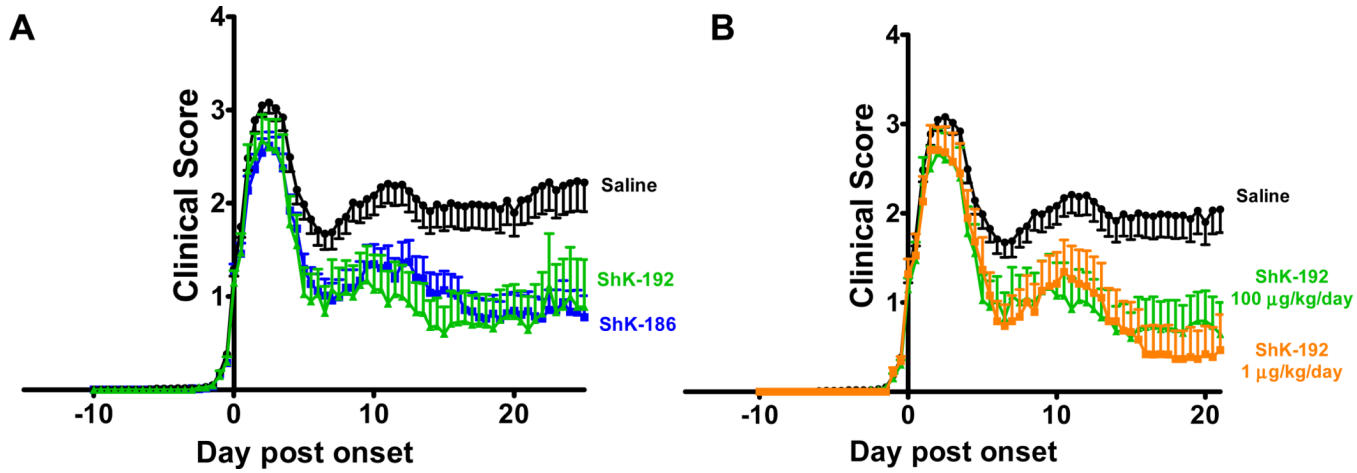

Figure 7. ShK-186 and ShK-192 reduce disease severity in chronic relapsing-remitting experimental autoimmune encephalomyelitis in DA rats

A, Effect of vehicle-, ShK-186- and ShK-192-treatment in rats with CR-EAE. ShK-186 and ShK-192 were administered by once daily subcutaneous injections, both at 100 µg/kg/day). Treatment was started at the onset of disease (clinical score=1). Cumulative p value from repeated measures two-tailed ANOVA for both ShK-186 and ShK-192 is $p<0.001$. **B,** Effect of treatment with ShK-192 at 100 and 1 µg/kg/day in rats with CR-EAE (cumulative $p < 0.001$). *Clinical scores*: 0.5=distal tail limp; 1=loss of tail tone; 2=mild paraparesis and ataxia; 3=moderate paraparesis, tripping while walking; 3.5=one hind limb paralyzed; 4=complete hind limb paralysis; 5=complete hind limb paralysis and incontinence; 6=moribund, difficulty breathing, does not eat or drink, euthanized immediately.

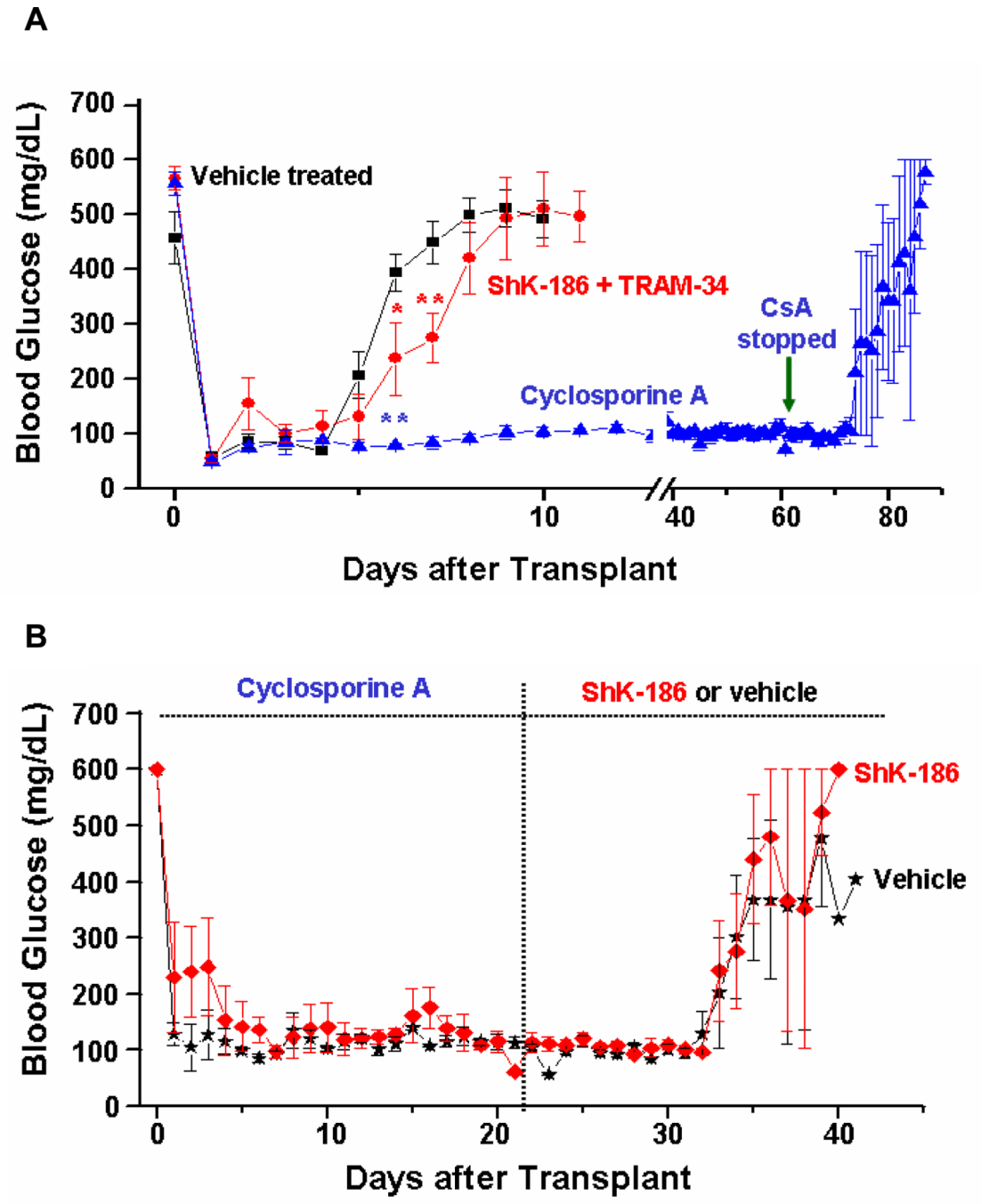

Figure 8. Effectiveness of ShK-186, TRAM-34 and cyclosporine A in preventing the rejection of transplanted pancreatic islets

A, Blood glucose levels from diabetic dark agouti (DA) rats transplanted with pancreatic islets from Lewis rats under the kidney capsule, that received either vehicle, ShK-186 (300 μg/kg twice daily s.c.) + TRAM-34 (20 mg/kg twice daily i.p), or cyclosporine A (5 mg/kg. s.c.). Cyclosporine A was stopped on day-60. Red *: $p<0.01$. Blue *: $p < 0.001$. Only two blue * are shown next to the cyclosporine A data, but every day thereafter until day 60 was statistically significant at $p < 0.001$. **B,** Blood glucose levels from transplanted DA rats that were treated with Cyclosporine A for 21 days followed by ShK-186 (100 μg/kg/day) or vehicle. DA rats were made diabetic by Streptozotocin (20 mg/kg, i.p., administered a total

of 5 times every 3rd day). Freshly isolated islets (4000IEQ) from Lewis rats were transplanted under the kidney capsule of DA rats 21 days after they developed diabetes mellitus (two consecutive readings of over 350 mg/dL of blood glucose was considered to be indicative of diabetes). Rats became euglycemic following islet transplant. The recurrence of diabetes was considered a sign of graft rejection.

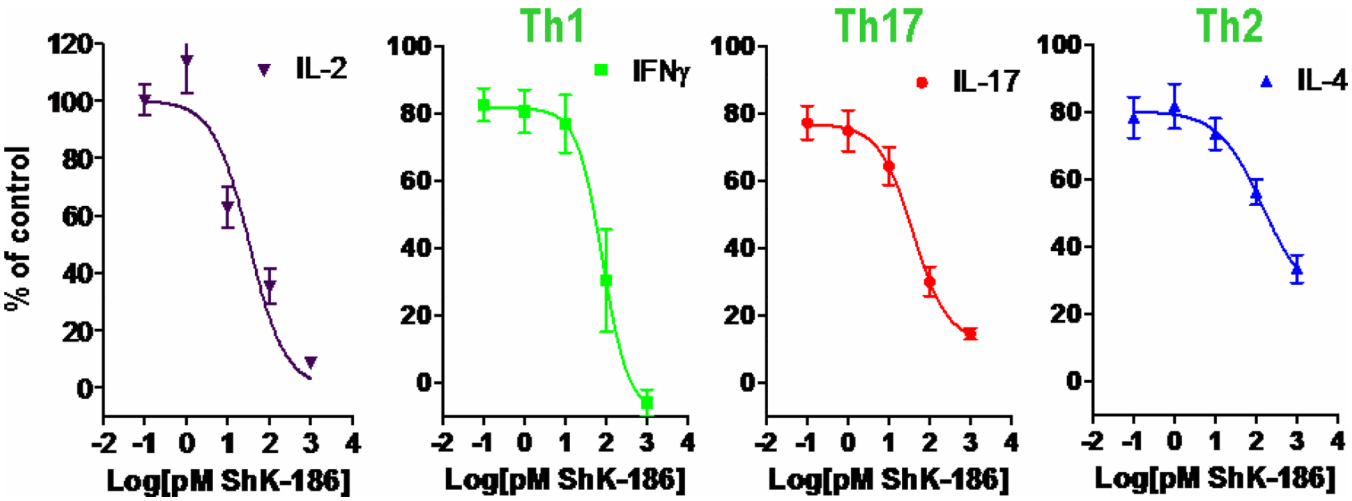

Figure 9. ShK-186 suppresses cytokine production in human T cells from whole blood

T cells were stimulated with thapsigargin, an inhibitor of the ER SERCA pump. ShK-186 was most effective in suppressing the production of IL-2 and the Th1 cytokine IFN-γ. It was less effective in suppressing IL-17 (Th17 cells) and least effective in inhibiting IL-4 (Th2 cells).

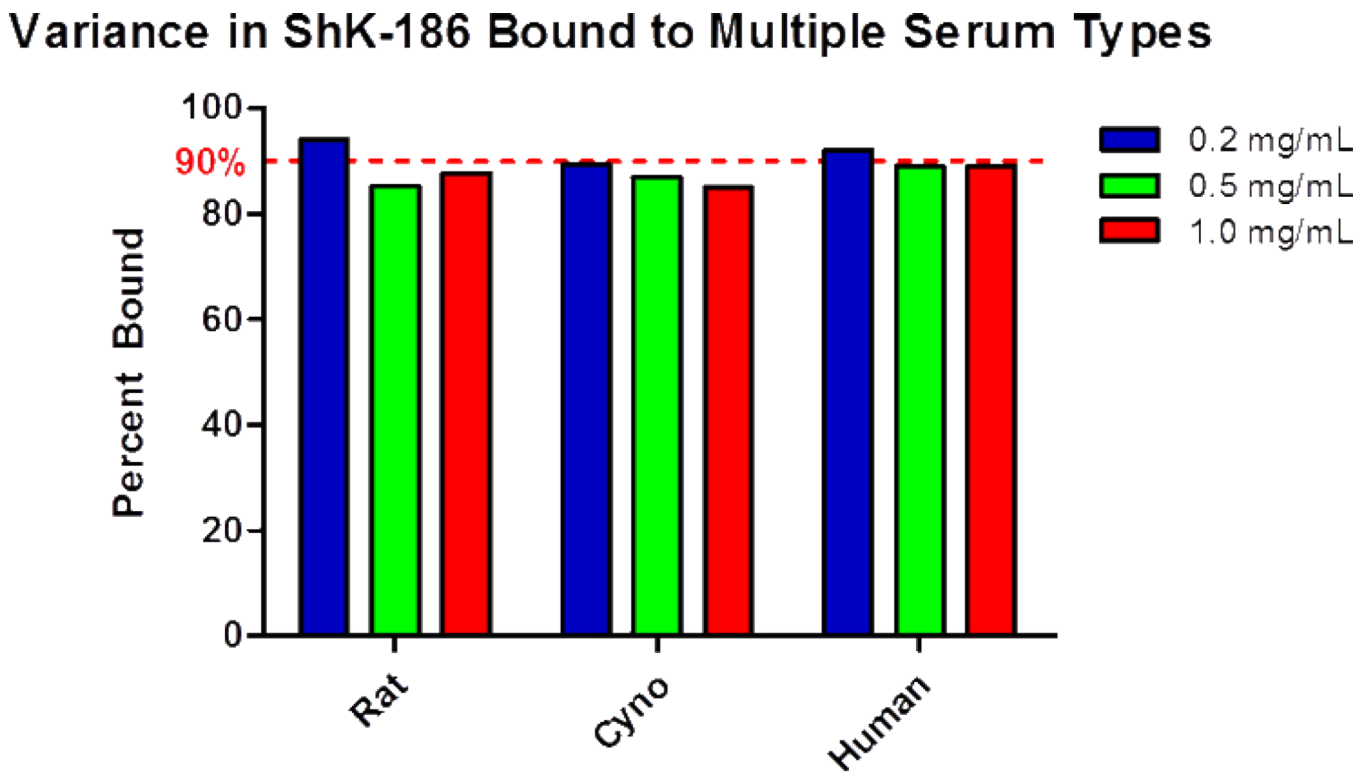

Figure 10. ShK-186 exhibits significant binding (90%) to proteins in human, rat (Sprague-Dawley) and Cynomolgus monkey serum

Sera were incubated for 15 min at room temperature with ShK-186, before being subjected to ultrafiltration (Millipore Centrifree Ultrafiltration Device - Cat#: 4104) followed by RP-HPLC. The sera were spiked with 1X or 10 µL/ml Halt™ Protease and Phosphatase Inhibitor cocktail and 1X or 10 µl/ml EDTA (0.5 M) to prevent dephosphorylation of ShK-186.

Table 1

Number of Kv1.3 and KCa3.1 channels per cell in T cells (A) and B cells (B) from different species.

A

Species	Channel Type (Channels/cell)	Naïve $CCR7^+CD45RA^+$		T_{CM} $CCR7^+CD45RA^-$		T_{EM} $CCR7^-CD45RA^-$	
		Resting	Effector	Resting	Effector	Resting	Effector
Human (CD4+ and CD8+)	Kv1.3	200–250	300–350	250	300–400	200–300	1500–1800
	KCa3.1	<5	500–550	20	500–600	20–35	40–50
Rhesus Macaque	Kv1.3	75	250	105	~195	125	1085
	Kv1.3	5	200	7	190	15	16
Sooty Mangabey	Kv1.3	235	~190	237	200	~230	1370
	KCa3.1	5	195	6	200	10	24
Rat	Kv1.3	5	200	5	200	50	1500
	KCa3.1	15	300	15	300	10	60
Mouse	Kv1.3	10–30	500	10–30	500	300	800
	KCa3.1	10	150	10	150	130	400
Dog	Kv1.3	180	~195	NT		NT	
	KCa3.1	~5	~150				

B

Species	Channel Type (Channels/cell)	Naïve (IgD^+CD27^-)		Early Memory (IgD^+CD27^+)		Class-switched memory (IgD^-CD27^+)	
		Resting	Activated	Resting	Activated	Resting	Activated
Human	Kv1.3	100	90	255	180	2425	3170
	KCa3.1	5	595	10	700	65	70

Table 2

The blocking potencies (K_d values) of ShK and selected analogs on a panel of K^+ channels is shown. For comparison, K_d values for two other Kv1.3 blockers, OSK1-(K16,D20) (Mouhat et al., 2005) and PAP-1 (Schmitz et al., 2005) are shown.

Channel	ShK (K_d: nM)	ShK-Dap^{22} (K_d: nM)	ShK-170/ ShK-186 (K_d: nM)	ShK-192 (K_d: nM)	ShK-Q16K-PEG[20K] (K_d: nM)	OSK1-(K16,D20) (K_d: nM)	PAP-1 (K_d: nM)	Clofazimine (K_d: nM)
Kv1.1	0.028	1.8	7	22	997	0.40	65	>10,000
Kv1.2	10	39	48	>100	639	3	250	>10,000
Kv1.3	0.010	0.023	0.069	0.140	0.94	0.003	2	300
Kv1.5	>100	>100	>100	>100	>10000	>100	45	>10,000
Kv1.6	0.2	10.5	18	10.5	466	>100	62	ND
Kv1.7	>100	>100	>100	ND	>10000	>100	98	ND
Kv2.1	ND	ND	>100	ND	ND	ND	3000	ND
Kv3.1	>100	>100	>100	ND	ND	>100	5000	>10,000
Kv3.2	5	ND	20	4.2	ND		980	ND
Kv11.1 (HERG)	>100	ND	>100	>100	>10000	>100	5000	ND
Kir2.1	>100	ND	>100	ND	ND	ND	15000	ND
KCa2.1	>100	ND	>100	ND	ND	>100	10000	ND
KCa2.3	>100	ND	>100	ND	ND	>100	5000	ND
KCa3.1	28	>100	115	>100	>10000	>100	10000	ND